

Cortical Auditory Functional Activation By Cortico-Striato-Thalamo-Cortical Circuits

by

Alejandro Parga Becerra

A Dissertation Presented in Partial Fulfillment
of the Requirements for the Degree
Doctor of Philosophy

Approved November 2014 by the
Graduate Supervisory Committee:

Janet Neisewander, Co-Chair
Ronald Hammer, Co-Chair
Amelia Gallitano-Mendel
Jim McLoone
Jie Wu

ARIZONA STATE UNIVERSITY

December 2014

ABSTRACT

Auditory hallucinations are a characteristic symptom of schizophrenia. Research has documented that the auditory cortex is metabolically activated when this process occurs, and that imbalances in the dopaminergic transmission in the striatum contribute to its physiopathology. Most animal models have focused the effort on pharmacological approaches like non-competitive N-methyl-D-aspartate (NMDA) receptor antagonists to produce activation of the auditory cortex, or dopamine antagonists to alleviate it. I hypothesize that these perceptual phenomena can be explained by an imbalance activation of spiny projecting neurons in the striatal pathways, whereby supersensitive postsynaptic D2-like receptor, signaling in the posterior caudatoputamen generates activation of the auditory cortex. Therefore, I characterized the neuroanatomical component involved in the activation of the auditory cortex. I evaluated the participation of dopamine D2-like receptor using selective dopamine antagonist manipulations and identified the circuits related to the auditory cortex by retrograde trans-synaptic tracing using pseudorabies virus (PRV-152). My results show that dopamine infused in the posterior caudatoputamen dose dependently increases the transcription of the immediate early gene, *zif268* in the auditory cortex, predominantly in layers III and IV, but also in cortical columns, suggesting enhanced functional auditory activity. This indicates the participation of the posterior striatum in the modulation of the secondary auditory cortex. I was able to demonstrate also that a coinfusion of a selective dopamine D2-like receptor antagonist, eticlopride and dopamine, attenuate the activation of the auditory cortex. Furthermore, using PRV-152 I delineate the distinctive circuit by axial mapping of the infected neurons. Thus, I found secondary projections from the posterior caudatoputamen

that synapse in the thalamus before reaching the auditory cortex. These striatal projections correspond to the same brain region affected by dopamine during auditory cortical activation. My results further characterized a mechanism to generate intrinsic perception of sound that may be responsible for auditory hallucinations. I propose this paradigm may elucidate insight on the biological basis of psychotic behavior.

ACKNOWLEDGMENTS

The present work would have not been possible without the motivation of my patients from the Psychiatric Hospital San Camilo, the Clinic San Juan de Dios and the military base La Arandia. I want to specially thank Jorge for sharing his words about residual schizophrenia, and Mauricio Rodriguez for his support throughout the program. I would also like to thank Dr. Hammer and the laboratory members as well as the staff of Basic Medical Sciences at the University of Arizona and the department of Neuroscience at Arizona State University.

TABLE OF CONTENTS

	Page
LIST OF TABLES.....	viii
LIST OF FIGURES	ix
PREFACE	x
CHAPTER	
1 INTRODUCTION	1
1.1 Statement of Purpose	1
1.2 Scope.....	3
2 BACKGROUND LITERATURE	5
2.1 History of Schizophrenia	5
2.2 Epidemiology	6
2.3 Clinical Definitions And Diagnosis	8
2.3.1 Course Of The Disease.....	9
2.4 Auditory Hallucinations	11
2.4.1 Brain Activity During Auditory Hallucinations	12
2.5 Antipsychotics Drugs.....	13
2.5.1 Mechanisms Of Conventional Antipsychotics	15
2.5.2 Mechanisms Of Atypical Antipsychotics	17
2.6 Dissociative Anesthetic Drugs.....	21
2.7 Dopamine	22
2.7.1 Dopamine Receptors	23
2.8 Basal Ganglia	24

CHAPTER	Page
2.8.1 Striatal Circuits	25
2.9 Mechanism For Intrinsic Auditory Activation	28
3 DOPAMINE-INDUCED AUDITORY CORTICAL ACTIVATION AND ATTE- NUATION BY D2-LIKE RECEPTOR-SELECTIVE ANTAGONIST IN THE CAUDATOPUTAMEN OF THE RAT	30
3.1 Project Summary	30
3.2 Introduction	31
3.3 Experimental Design.....	33
3.3.1 Striatal Dopamine Dose Dependent Study.....	34
3.3.2 Laminar Assessment Of The Auditory Cortex.....	34
3.3.3 Coinfusion Of Dopamine Antagonists And Dopamine	34
3.3.4 <i>Zif268</i> Probe Labeling	35
3.3.5 tissue Preparation And Ishh	35
3.3.6 Image Analysis	36
3.3.7 Statistical Analysis	37
3.4 Results.....	38
3.4.1 Localization Of Infusion Sites	38
3.4.2 Sound And Dopamine Dose Dependently Increase Expression Of <i>Zif-268</i> mRNA In Auditory Cortex.....	39
3.4.3.... Dopamine Selective Antagonist Attenuate Dopamine Induce Auditory Activation.....	51
3.5 Discussion	53

CHAPTER	Page
3.6 Financial Disclosures	55
4 TRANS-SYNAPTIC RETROGRADE TRACING OF AN AUDITORY CORTICAL CIRCUIT FROM THE POSTERIOR CAUDATOPUTAMEN	56
4.1 Project Summary	56
4.2 Introduction	57
4.2.1 Tracing Of Neuronal Circuits	58
4.3 Experimental Design.....	59
4.3.1 Animals	59
4.3.2 Virus.....	60
4.3.3 Experimental Paradigm	60
4.3.4 Intracerebral Injections.....	61
4.3.5 Tissue Processing.....	62
4.3.6 Fluorescent Imaging.....	63
4.3.7 Analysis Of Tissue	63
4.3.8 Circuit Reconstruction.....	64
4.3.9 Mathematics And Equations	66
4.4 Results.....	66
4.4.1 Time Of Detection For Regions Of Interest.....	67
4.4.2 Primary And Secondary Projections.....	68
4.5 Discussion	74
4.6 Financial Disclosures	80
5 DISCUSSION	81

CHAPTER	Page
5.1 Conclusion.....	86
LITERATURE CITED.....	88

LIST OF TABLES

Table	Page
1. P Values Of Planned Comparisons Of The <i>Zif268</i> mRNA Expression	41
2. ANOVA and Bonferroni's test hypothesizing equal functional activation	43
3. Kruskal-Wallis test hypothesizing similar functional activation in brain regions by cortical layers	44
4. MANOVA And Bonferroni Adjusted F-Statistic In Temporal Cortex	49
5. P Values Of MANOVA And Bonferroni Adjusted F-Statistic In Motor Cortex	50
6. Rostrocaudal Brain Segment Assessed For ROI	64
7. Comparison Of The Synaptic Ranks Between ROI Detected	72
8. Logarithm Of The Average Cell Counts For Brain Regions	73

LIST OF FIGURES

Figure		Page
1.	Diagram Of The Main Brain Regions Related To The Auditory CSTC.....	26
2.	Target Region And Injection Site	38
3.	A. Examples Of Hemisections From Treatment Groups	39
3.	B. Mean Expression Of The <i>Zif268</i> Mrna In The Auditory Cortex.....	40
3.	C. Inter-Hemispheric Comparison Of <i>Zif268</i> Mean Expression	41
4.	Functional Activation By Sound, Dopamine, Light And Saline Treatments	39
5.	Mean Expression Of <i>Zif268</i> Mrna At Six Rostrocaudal Levels	47
6.	A. Examples Of Hemisections From Treatment Groups	51
6.	B. Mean Expression Of <i>Zif268</i> Mrna In Auditory Cortex	52
7.	Time Line Of Post-Inoculation Times Evaluated.....	61
8.	A. Cell Expressing eGFP In The First Synaptic Rank.....	67
8.	B. Injection Site And Ipsilateral Cortex	68
8.	C. Primary Projections To Auditory Cortex	69
8.	D. Close-Up Of Cells Expressing eGFP In The Striatum.....	70
8.	E. Cells Expression eGFP In The Second And Third Synaptic Level	71
9.	A. Brain 12 Hours Postinoculation	77
9.	B. Brain 36 Hours Postinoculation	78
9.	C. Brain 48 Hours Postinoculation.....	79

PREFACE

Manifestations of psychotic symptoms like auditory hallucinations are an interesting ground for research of the neurobiological basis of auditory perception. Our understanding of antipsychotics as a model to attenuate endogenous function of the brain, and the neuroanatomical knowledge provided by neuronal tracers allow the identification of neuronal networks responsible for these psychotic manifestations. Therefore, the present work evaluates the pharmacological effect of increased dopamine in the posterior caudatoputamen and test the effect of a selective D2-like receptor antagonist in the activation of the auditory cortex. This activation was assessed at the level of cortical structure to point out the exact location of the effect in the auditory cortex. In this manner, the efferent projections towards the highlighted area in the auditory cortex were retrogradely traced to establish the multisynaptic circuit involved. Studying the networks related to these phenomena will allow a better understanding of the mechanisms that lead the brain to generate a false perception of sound and may provide insight of the neuronal source of inner speech.

CHAPTER 1

INTRODUCTION

1.1 Statement of Purpose

I am a neuroscientist with a medical background interested in the neurobiological basis of perception and its alterations in psychiatric disorders such as schizophrenia. My main motivation to pursue studies in neuroscience is my fascination for the sophisticated circuitry that recreates inside the brain a perception of our surroundings and us. My research focuses on the neuromodulation of cortico-striato-thalamo-cortical (CSTC) circuits relevant to the physiopathology of auditory hallucinations. These distortions of auditory perception produced by psychostimulants or psychotic disorders provide an interesting groundwork to study endogenous perception of the auditory modality.

To achieve my research objectives I joined the laboratory of Dr. Ron Hammer, where I developed my dissertation project. The main hypothesis of my research was based on three pieces of evidence. The first one is the increased dopaminergic transmission in the caudate nucleus shown by patients with schizophrenia; the second one relates to the therapeutic effects of antipsychotics through D2-like receptors; and the third one is the description of corticostriatal projections from the auditory cortex.

My research evaluates dopaminergic transmission in the dorsal caudatoputamen of the rat as endogenous factor that activates the auditory cortex. I used stereotaxic intracranial procedures to infuse dopamine or co-infuse D2-like selective dopamine receptor

antagonist in the posterior aspect of the caudate nucleus. In this manner, I was able to demonstrate a dopamine-dependent activation of the auditory cortex quantifying changes in the expression of the messenger RNA of *zif268*, an immediate early gene linked to neuronal activity. This pharmacological work was presented in the Annual Scientific Conference of the Society of Biological Psychiatry (SOBP), where I was nominated for best presentation because of its ability to translate basic science into concrete clinical applications.

In my research I also describe the brain regions that participate in the neuronal circuit responsible for dopamine induced auditory activation. Using pseudorabies virus 152, a trans-neuronal retrograde tracer that expresses enhanced green fluorescent protein as a marker for trans-synaptic infection, I was able to map multisynaptic projections to the auditory cortex that originated in the posterior caudate. These circuits constitute a neurobiological measure that relates to a mechanism of psychopathology. Our findings contribute; therefore, under the current research domain criteria promoted by the National Institute of Mental Health, to define the units of analysis under the construct of network disruptions of brain connections. This project provides a new piece of evidence related to the existence of an auditory cortico–striato-thalamo-cortical (CSTC) circuit relevant to the physiopathology of auditory hallucinations.

Making use of these findings, I look forward in my career to characterizing the role striatal pathways play in the auditory CSTC circuit. I believe it is in these networks of the basal ganglia, where information decoded from the auditory sensory system is fitted to schemata that contain our perspective of the world. Classically, the striatal pathways are

described as direct and indirect, with both pathways integrated at the globus pallidus level. In theory, the glutamatergic corticostriatal input they receive generates an activation that loops back to the cortex through the thalamus. My strategy consists in assessing each portion of the auditory CSTC circuit using recombinant vectors that would allow controlling for neuronal populations, hence permitting to elucidate functioning patterns at each level of the circuit. A matter for future research is to study endogenous inputs to the auditory cortex implementing neuroimaging and electrophysiological techniques. Decoding the function of the auditory CSTC circuit will add to our understanding of the physiopathology of auditory hallucinations and would assist in the development of more accurate interventions for psychotic symptoms.

1.2 Scope

Schizophrenia is a conglomerate of mental disorders with diverse clinical course and a broad effects in multiple brain functions, which include disturbances of thinking and perception, affect and social behavior. The onset of the disease occurs at the beginning of adulthood and the prognosis depends on the cognitive and social dysfunction developed over the time. Low adhesion to treatment strategies and profound side effects of antipsychotics usually generate patients with high dysfunctional lifestyle; therefore, schizophrenia is a major concern in public health worldwide Barbato (1996). Beyond the comorbidity and social cost of schizophrenia, the disease provides a fascinating scenario to study the source of endogenous sound perception (Waters et al., 2006).

In psychotic disorders, hallucinations can have complex sensory components. The visual and somatosensory modalities may participate in these phenomena, though verbal auditory hallucinations are most frequent in the description to the physician (Lecrubier et al., 2007). The effects on brain circuits involved in auditory perception leading to a false sound perception emphasize that research on these phenomena may provide a mechanism of intrinsic perception of sound that not only bring insight of the physiopathology of the disease but also show the brain interaction that allows us to generate thought and interpret the world.

CHAPTER 2

BACKGROUND LITERATURE

2.1 History of Schizophrenia

Bleuler first named schizophrenia in 1908, and since its diagnosis has depended on the clinical anamnesis. The word comes from the greek roots schizo-phrene, which mean split- mind. Patients with schizophrenia usually have a heterogeneous manifestation composed of three arrays of symptoms: positive, negative and cognitive (Liddle, 1987), which depict the excitation or inhibition of different neuronal networks.

There have been descriptions of psychotic symptoms since the times of ancient Egypt. Although the population has been aware of mental illness throughout history, it was not until a description by Kraepelin in 1887 that schizophrenia could be differentiated from other mental disorders. In his description Kraepelin referred to the disease as dementia praecox, an early onset compared to other types of dementia characterized the syndrome that will be better characterize in 1911 by Bleuler.

Initially, some major features seen in schizophrenic patients were classified into paranoid, disorganized, and catatonic. These subtypes were later included in the Diagnostic and Statistical Manual of Mental Disorders (DSM-III) with the addition of the residual and undifferentiated subtypes. The evaluation of clinical observations has changed over time allowing for few modifications in the DSM-IV and recently DSM-

V, but a biological basis for schizophrenia is still elusive from the clinical classification. This has led to a low correlation of prognosis and the appropriate therapeutic for each subtype. As a result, the National Institute of Mental Health proposed an initiative to reclassify the symptomatology of schizophrenia following units of study from genes to behavior under the constructs of mental systems involved (Miller, 2010). This approach called research domain criteria allows a better match to our understanding and focus research into a more effective classification of the disease.

2.2 Epidemiology

It is estimated that 29 million patients have schizophrenia of which only 9 million are located in developed countries. Such difference in the distribution has been explained by factors that affect the prevalence since an incidence of 0.1 to 0.4 cases per 1000 people is consistent in different regions despite socioeconomical variables (Jablensky et al., 1992); thus, the effect of health care, minority groups and access to development shows a lifetime prevalence that varies between 1 to 18 cases per 1000 people worldwide (Warner, 1995). Places with wider variation in the prevalence of schizophrenia also showed a long-term decrease as developing countries provide better care that improves the outcome of patients (Warner, 1995). Places with wider variation in the prevalence of schizophrenia also showed a long term decrease as developing countries provide better care that improves the outcome of patients (Leff et al., 1992). As a result, symptomatic treatment for schizophrenia may improve

symptoms in places of high prevalence though the cause of this disorder is still not tackle by any of the current therapeutics.

An accurate estimation of the costs can only derive from reliable data in developed countries. In the United States, a total annual cost of \$32.5 billion that accounts for \$17.3 billion of direct cost, \$12 billion of indirect cost and \$3.2 billion in other related costs (Knapp et al., 2004). Those figures depict the immense impact of schizophrenia in society.

Risk factors for schizophrenia can be group into sociodemographic, predisposing and precipitating aspects of the disease. They show the role of social environment in the manifestation of psychotic episodes. In the sociodemographic factors, unmarried individuals have four times a higher risk of presenting psychotic episodes. In addition, a lower social class has a strong correlation in western countries with schizophrenia. The genetic component while still elusive is the predisposing factor of more relevance. Recent research demonstrates that at least 17 different genotypes contribute to the disease, which result in the expression of eight phenotypes sets. The association and interaction between the genotypes and phenotypes seems to contribute for up to 60% of cases (Arnedo et al., 2014). Some other insults like birth complications have shown a lower correlation to explain the disease. On the precipitating factors a less supportive family with negative affective interactions and fragmented communication are the most relevant not only for initiating a first psychotic episode but also in relapse and chronic manifestations (Miklowitz, 1994).

2.3 Clinical definitions and diagnosis

The DSM has presented different characterizations of the disease. The latest version, DSM-5, attempts in this manner to bring research domain criteria to allow understanding of the disorder based on the neuropathology (Bhati, 2013). Thus, the differential diagnosis of schizophrenia requires considering six criteria:

A. The characteristic symptoms like delusions, hallucinations, disorganized speech, disorganized or catatonic behavior and negative symptoms like affective flattening, alogia and avolition must be predominant for more than a month with at least two of them present to fulfill criterion, or less if successfully treated (APA, 2013)

B. Social and occupational dysfunction is another criterion whether loss of self-care, interpersonal relations or work activities from the level previously accomplish, or in the case of early onset schizophrenia the lack of achieving the level according to the current age of onset.

C. Duration of six month is required where symptoms fluctuate between positive, negative or cognitive symptoms.

D. Exclusion criteria include:

a. Mood disorders during the onset of the disease must be evaluated as some major mood disorders or schizoaffective disorder may manifest similar clinical frames.

This particular exclusion denotes how some patients have a disease that involves circuits relevant to other brain functions like amygdala.

b. Substance abuse or medications that produce psychotic acute syndromes are other consideration for differential diagnoses. Most of these drugs are psychostimulants like phencyclidine or ketamine, which may reproduce similar case by enhancing cortical activation (See section on psychostimulants)

c. Global developmental delay or Autism spectrum disorders are other differential diagnosis. Schizophrenia could be considered in this case additional diagnosis when predominant delusions or hallucinations step on the previous diagnosis.

2.3.1 Course of the disease

The first consultation usually appears during the manifestation of a positive phase that entails delusions, hallucinations, disorganized speech or catatonic behavior. The course of the disease continues with negative phases that are normally composed by affective flattening, alogia or avolition. The presence of these negative symptoms is associated with the disease detriment in cognitive function characterized by lack of attention, executive function and problems with working memory (McGorry et al., 2002). Symptoms of this nature appear combined in most cases given the disease multistage record; nevertheless, poor prognosis is related to accentuate negative phases and an early onset of the disease (Rund, 1998). In this manner, the manifestations vary between a paranoid phase characterized by positive symptoms, a disorganized phase with cognitive detriment, an undifferentiated phase composed of a mix of positive and negative symptoms and a residual phase where negative symptoms are predominant. These clinical phases may vary in their intensity or according the patient's response to treatment. The

current estimate of medium-term course shows 45% recover after the initial episode, 20% have a constant phase that do not improve and 35% have a fluctuating disease course with periods of remission and illness.

The duration of an acute stage may vary between patients as well as the frequency of these episodes, which are present throughout a lifetime. In many cases, there is a prodrome stage, where positive symptoms are not pronounced, and in which diagnosis has proven elusive. Although negative symptoms precede frequently cognitive deficit, vocational and social disabilities of patients are predicted by cognitive dysfunction having a short-term memory detriment and attentional deficit a main participation (Green, 1996). The content of positive symptoms is associated with the level of education, which may produce sophisticated delusions or hallucinations described as Schneider's first rank symptoms (Crow, 1980). Different cultural backgrounds may initially disclose other mental affections as major complaint covering the actual beginning of the disease, which can start as early as six years of age. Nonetheless, 70% of cases present auditory hallucinations, which make of this symptom important tool for diagnosis (Barbato, 1996). Therefore, the clinical features of auditory hallucinations are relevant to evaluate the kind of brain insult that generates these phenomena; therefore, research in auditory hallucinations may also uncover the brain regions and synaptic changes underling the neuropathology of schizophrenia like symptoms.

2.4 Auditory hallucinations

The false perception of sound described in psychiatric cases, as an additional voice perceived separated from the mental process is the most common way of presentation. However, other mental disorders that can exhibit auditory hallucinations are bipolar disorders with a 20-50% prevalence and posttraumatic stress disorder with 40% prevalence (Choong et al., 2007). Location, self-other attribution and language complexity are the clinical aspects evaluated of auditory hallucination (Stephane et al., 2003). Other characteristics like duration, frequency and intensity that are part of the anamnesis assessment have not related to the brain regions affected. In this manner, the perceived location of the hallucination can clinically be described as the hallucination heard from outside the head of the patient or heard from the inside (Bleuler and Bleuler, 1986). The right temporoparietal junction has shown anatomical differences in these patients compared to healthy controls. Brain imaging studies have also shown changes in the left temporal cortex and Broca's area in patients with verbal auditory hallucinations (Silbersweig et al., 1995, Cuchia et al., 2008), while changes in the cingulate and temporal cortices are associated to self-other misattribution (Hubl et al., 2004, Allen et al., 2007). Research on the neuroanatomical input of the auditory cortex has shown two different pathways one ventral and another dorsal (Rauschecker and Tian, 2000). The parietal region and superior temporal gyrus appear to be the coalescent point for both pathways (Altmann et al., 2007). Based on these findings the secondary auditory, prefrontal, cingulate, subcortical regions demonstrated changes in patients with auditory hallucinations (Allen et al., 2008). The limitations to the study in human brain and the

nature of subcortical regions makes this area to remain unclear; however, the bilateral thalamus, right putamen and caudate, bilateral parahippocampus, cingulate and orbitofrontal cortex appear to be associated with auditory hallucinations (Silbersweig et al., 1995).

2.4.1 Brain activity during auditory hallucinations

The functional study of the brain utilizes non-invasive procedures to evaluate the electric activity of the brain. For example, electroencephalographic variations or the oxygenation level in blood like in the functional MRI and PET are used to assess the level of metabolic activity of the nervous tissue (Font et al., 2003). In animal models, techniques with higher resolution and greater detail have been used to evaluate the expression of functional markers in the tissue and the electric activity of the neurons in specific brain regions.

Human studies evaluated the activity of brains during hallucinations or their performance on verbal task compared with healthy controls (Lahti et al., 2006). From these studies, the temporal cortex is consistently highlighted and has shown that different regions of the temporal cortex are responsible for different features of sound. For example, Alemann et al. using electroencephalographic recordings suggested that the anterior aspect of the superior temporal lobe has a role in sound identity while the posterior aspect is in charge of the spatial processing. In animal models, aberrant dopaminergic transmission seems to play an important role (Carlsson, 1988). The interaction between auditory related regions on animal models suggests lack of cerebral

inhibition and abnormal excitation during auditory hallucinations (Weiss and Heckers, 1999). It has been suggested, therefore, that the cortical activity provides the specific signal information of the perceptual content whereas activity in deep brain structures may modulate recognition of auditory patterns or produce auditory hallucinations (McGuire et al., 1995).

The treatment of auditory hallucinations depends on the interference and intensity of these phenomena in normal life, as well as other clinical manifestations that accompanied it in psychotic and organic conditions like trauma and tumors. When auditory hallucinations are intrusive and require control, antipsychotics are the usual treatment (Shergill et al., 1998) though transcranial magnetic stimulation has been used as adjuvant (Hoffman et al., 2005, Aleman et al., 2007). These measures address in part the modulation of the activity in the auditory cortex and language cortical regions; nevertheless, the action of antipsychotics is been debated since they are systemically administer acting in various brain regions and they have multiple receptors sites.

2.5 Antipsychotic drugs

The use of antipsychotics started in 1952 with the use of chlorpromazine in the Central Military Hospital by Drs. Hamon, Paraire and Velluz as well as in the Sainte-Anne Hospital by Dr. Deniker and Harl (Lopez-Munoz et al., 2005). This phenothiazine, synthesized by Charpentier in 1950 was initially used as anesthetic (Swazey, 1979). The search for antimalarial compounds in World War II had led to the implementation and synthesis of aminoalkyl chains (Gilman and Tolman, 1946). These antihistamines

developed as antimalarial drugs found good use as adjuvant for anesthesia before their antipsychotic effects were described by Laborit and Huguenard in 1951 (Laborit and Huguenard, 1951). More than forty phenothiazines were developed since 1960s by Rhône-Poulenc, but only fluphenazine and haloperidol were available in the US (Shen, 1994). Due to the side effects, especially extra pyramidal symptoms, clozapine was developed in Switzerland by Wander Pharmaceuticals (Hippius, 1989); however, prescription was limited due to the report of agranulocytosis as side effect (Bailey, 1997). In this manner, other drugs derivate from the latter class of antipsychotics were developed. These, atypical antipsychotics work through mixed receptor antagonism and produce low extra pyramidal symptoms.

Most treatments that have demonstrated effectiveness alleviating psychotic symptoms have effects on the dopaminergic transmission in the brain. Specifically, the D2-like receptors in the mesolimbic and nigrostriatal brain areas (Seeman et al., 1975). Clinical treatment schemes show improvement in 75% of acute patients over 6-14 weeks with 300-750 mg of chlorpromazine equivalents (Dixon et al., 1995); thus, these medications help to improve symptoms and prevent recurrence of acute psychotic syndromes (Lewis and Lieberman, 2000). Nonetheless, 30% of acute patients will not response to antipsychotics, and 60% of chronic patients will not have improvement on negative and cognitive symptoms (Miyamoto, 2002).

This family of drugs has grown in recent years leading to their classification into conventional and atypical antipsychotics. Conventional antipsychotics come from five groups of molecular structures Phenothiazines, Thioxanthenes, Butyrophenones,

Dibenzoxazepines and Dihydroindolones, which block dopamine receptors as a mechanism of action (Freedman, 2003). These medications also share side effects in different systems that involve in the central nervous system sedation and extrapyramidal symptoms like tremors, dystonias, akathisia, akinesia, stiffness and shuffling gait. Endocrine side effects like amenorrhea, galactorrhea, ginecomastia and weight gain. Anticholinergic effects like constipation, blurred vision and dry mouth. In addition, skin and eye side effects like cutaneous rash, phototoxic skin reaction and granular deposits in the cornea (Lieberman et al., 2005). Consequently, newer antipsychotics attempt to eliminate these side effects acting in other neuromodulators besides dopamine receptors or having a more selective interaction with dopamine.

The current indication for conventional antipsychotics is patients that respond with few side effects, and those that will require short or long intravenous medication.

Nonetheless, chronic treatments will require higher doses due to up-regulation of D2-like dopamine receptors (Florijn et al., 1997, Kapur et al., 2000) and adjuvant medications to control comorbidity. As atypical antipsychotics become available in other ways of administration besides of the oral route, the tendency is to use atypical antipsychotics as first line of treatment.

2.5.1 Mechanisms of conventional antipsychotics

The mechanism of conventional antipsychotics brought research to evaluate the presynaptic and postsynaptic targets of these molecules. In the first scenario, the hypothesis that antipsychotics may affect at the presynaptic level the release of dopamine

was first study by Seeman & Lee in 1974. They found in nerve terminals that the dose of haloperidol necessary to increase dopamine release was a hundred times more than the clinical concentration measure in cerebrospinal fluid (1 – 4 nM), and that chlorpromazine, a more potent antipsychotic required a thousand times the observed clinical dose. Moreover, the presynaptic effect of antipsychotics to block the release of dopamine also requires higher doses of approximately ten times of those observed in the spinal fluid. In this way, the role of antipsychotics in modifying the release of dopamine with a presynaptic target was rejected.

Another hypothesis evaluated the action of antipsychotics in the postsynaptic portion of dopaminergic synapses. The effects on dopamine-stimulated adenylate cyclase were also rejected not only for the higher doses require but also because of the lack of correlation with the clinical potency. However, the relationship between clinical potency of antipsychotics and the displacement of the binding of [3H]-haloperidol provided the strong evidence that in striatal membranes there was a common target for all antipsychotics. This target was later confirm to be a dopaminergic receptor when the affinity of dopamine changed the binding of [3H]-haloperidol more than any other neurotransmitter. Likewise, a stereo-selectivity of this binding was assessed by comparing [3H]-haloperidol with [+] and [-] butaclamol, which does not have therapeutic effects though it bind dopamine receptors. With the use of more selective radioactive molecules, dopamine receptors were classified into two families D1-like and D2-like dopamine receptor (Kebabian and Calne, 1979) of which a dopamine D2-like receptors were the common target of the conventional antipsychotics (Seeman et al., 2002). The

exact location of the effect of D2-like receptors has brought more considerations as D2-like receptors were found to be in the presynaptic and postsynaptic sites (Bloom et al., 1965).

2.5.2 Mechanisms of atypical antipsychotics

The side effects produced by conventional antipsychotics favor the search for new agents with less extrapyramidal effects, dyskinesia and lower prolactinemia while greater therapeutic effects. Atypical antipsychotics still have other side effects; however, like weight gain, hyperglycemia and dyslipidemia. Their broad pharmacological profile is still under research, but these new drugs are commonly the first line of treatment in acute psychotic cases (Buckley, 2001, Kane et al., 2003, Miyamoto, 2003). Atypical antipsychotics target multiple neurotransmitters, which provide more mechanisms of action; therefore, we will consider them separately to see each profile.

D2 receptor antagonism: Benzamides have high affinity for D2-like receptors and low D1-like receptors. Part of these drugs are Amisulpride and sulpride, which show a presynaptic effect at low doses that generates release of dopamine, but a postsynaptic effect that associates with antipsychotic action at high doses. Benzamides are characterized for a fast dissociation of D2 receptors and prefer occupancy of limbic targets (Bressan et al., 2003). Amisulpride is indicated in acute phases at doses of 400 – 800 mg /day as well as in the management of negative symptoms with doses of 50 to 300 mg / day (Curran and Perry, 2001). Due to their action on D2-like receptors, benzamides are thought to stabilize the effects of endogenous dopamine toward striatum; therefore,

they are also used in the treatment of mood disorders like bipolar disorder and dysthymia. Common side effects of benzamides include extrapyramidal effects like dystonia, tremor, akathisia and parkinsonism. Less common side effects are hyprolactinemia, hypersalivation, anxiety and weight gain. Overdose of benzamides produce electrocardiographic changes like torsades de pointes. Due to their effects in the heart, benzamides should not be used in patients with long QT segment, low heart rate or hypokalemia. Benzamides are not metabolized in the liver, and excreted by the kidney in a 23 %– 46 %, they have interactions with other medicines like tricyclics and other antidepressants, and clozapine.

D2 receptor partial agonism: Aripiprazole has an interesting D2-like receptor profile because of the affinity for the receptor as agonist and antagonist. It also interacts with serotonin receptors having agonistic effects on 5-HT_{1A} and antagonist action on 5-HT_{2A} (Shapiro et al., 2003) as well as low affinity for histamine and cholinergic receptors. This has been studied in animal models where aripiprazole stabilizes the dopaminergic system through selective activation of D2-like receptors (Lawler et al., 1999). Evidence on aripiprazole is not consistent for long term use because in maintenance treatments with doses of 10 to 30 mg / day extrapyramidal symptoms are develop over time (Khanna et al., 2014). However, aripiprazole has also been used in major depression and autism because its ability as mood stabilizer. The liver metabolizes aripiprazole and medicines that affect the activity of CYP2D6 and CYP3A4 enzymes interfere with its bioavailability.

Serotonin receptor 5-HT_{2A} antagonism: clozapine and its derived drugs risperidone, olanzapine and ziprasidone are 5-HT_{2A} receptors antagonist. It is believe that these drugs increase the release of glutamate in prefrontal cortex (Aghajanian and Marek, 2000). The high occupancy of serotonin receptors by this compounds correlate with their therapeutic effects although all of them show some antagonist profile with D2-like receptors as well (Farde et al., 1995, Kapur et al., 1998). Clozapine is used as second line of treatment when symptoms are resistant in schizophrenia. It is also helpful in the treatment of schizoaffective syndrome as antipsychotics. The major side effect of clozapine is agranulocytosis, which occurs in 1 % of the patients regularly after three months of use. Therefore, the first six months patients taking clozapine need to have their blood counts checked. Other less frequent side effects of clozapine include cardiac toxicity, gastrointestinal hypomotility and hypersalivation. Interactions with quinolones and benzodiazepines prevent the use of clozapine with these medicines. The liver highly metabolizes clozapine through the cytochrome P450, therefore it has a first-pass metabolism that limits its bioavailability to 60 %. The dosage of clozapine varies between 12.5 to 400 mg per day. Due to the effects of clozapine in other neurotransmitter systems, its effects as antipsychotic not only depend on the serotonergic system; nonetheless, the improvement of cognitive and negative symptoms seem to be related to the facilitation of cortical glutamatergic release as outcome on other neurotransmitters.

Serotonin receptor 5-HT_{1A} partial agonism: These agents may reduce the release of glutamate on pyramidal cells (Aghajanian and Marek, 2000). Though they may contribute to mood disorders, in psychotic cases their pharmacological profile makes

them useful as adjuncts through potentiation of dopamine antagonists or decrease of extrapyramidal effects (Lucas et al., 1997). Azapirone and buspirone are used in the treatment of anxiety disorders and depression. Some side effects are restlessness and dizziness but do not present the potential for drug abuse or addiction as benzodiazepines or other mood stabilizers.

Modulation of glutamate receptors: Allosteric agonists of the NMDA receptor provide in animal models improvement of parameters for negative and cognitive symptoms (Goff and Coyle, 2001). There are four ways to affect the glutamatergic system: glycine reuptake inhibitors, glutamate reuptake inhibitors, metabotropic receptor agonists and AMPA/kainite receptor antagonist. The first and second ones are inhibitors of excitatory neurotransmitters, which may affect trafficking of glutamate receptors specifically in the prefrontal cortex, basal ganglia and hippocampus (Bergeron et al., 1998). The third mechanism refers to the presynaptic receptors mGlu group II, which regulate release of glutamate. Agonist of this group of receptors, especially mGluR5 decreases glutamate release and have antipsychotic activity (Rowley et al., 2001, Chavez-Noriega et al., 2002). Lastly, the AMPA/Kainate receptor antagonism has shown to improve deficits on working memory probably through increase of glutamate release (Svensson and Mathe, 2000). Nevertheless, the development of drugs for treatment use is still under research, in part due to the complex function of the NMDA receptor with multiple binding sites.

Norepinephrine receptors: Agonists of the alpha-2 postsynaptic receptor have demonstrated to improve cognitive deficits (Fields et al., 1988) through their action in the prefrontal cortex; therefore, clonidine or guanfacine have been used as adjuvant drugs in

the treatment of cognitive dysfunction. On the contrary, antagonists of the alpha-2 receptor like idazoxan enhance cortical release of dopamine reproducing the antipsychotic action of clozapine when it is administered in conjunction to dopamine antagonists (Millan et al., 2000).

Nicotinic acetylcholine receptors: Stimulation of these receptors in the prefrontal cortex improve cognitive function by acting on the alpha-7 subunit type (Rezvani and Levin, 2001) and also sensory gating through alpha-4-beta2 agonism (Schreiber et al., 2002). Muscarinic receptor agonists had antipsychotic action through M1 cholinergic receptor, which improves cognitive function, negative symptoms and affective disorders (Bymaster et al., 2002).

2.6 Dissociative Anesthetics Drugs

Other compounds that stimulate the glutamatergic system can cause schizophrenia-like symptoms. The interaction that some antipsychotics have with noncompetitive NMDA receptor antagonists has brought the hypothesis that this receptor may participate in the neuropathology (Olney and Farber, 1995). Therefore, phencyclidine (PCP) and ketamine are commonly used in animal models. They can reproduce correlates of the positive- and negative-like schizophrenia symptoms as well as cognitive deficits in standardized animal paradigms. The hypothesis has been tested on pharmacological models where 5-HT_{2A} antagonist recover the deficit on prepulse inhibition (PPI) induced by PCP; similarly to D2-like antagonist (Wang and Liang, 1998). In addition, 5-HT_{2A} antagonists recover the metabolic activation of prefrontal

cortex generated by ketamine (Duncan et al., 2003). Although the mechanism by which PCP and ketamine produce dissociative effects in humans and deficits in cognitive and sensory gating function is not well understood, a possible explanation attributes a high function of NMDA receptor in the prefrontal cortex; hence, the specific acute effect of NMDA antagonist in attenuating symptoms and improving the deficits in animal models (Coyle, 1996).

2.7 Dopamine

Kathleen Montagu first described dopamine in 1957, and its relevance in the brain came to light when it was found diminished in the brains of patients with Parkinson's disease (Ehringer and Hornykiewicz, 1960). This finding was later related to schizophrenia as patients receiving conventional antipsychotics developed Parkinsonism. In this manner, increased dopamine transmission in the striatum has been reported in schizophrenia patients with the use of radiotracers to evaluate the availability of D2-like receptors (Abi-Dargham et al., 2012). The action of dopamine has been related to motivation, reward and reinforcement of learning. This catecholamine is produced in the substantia nigra and ventral tegmental area of the brain. From these areas of the mesencephalon dopamine is released in the cortex and basal ganglia, of which the striatum is a major target. Dopamine is produced from tyrosine by the tyrosine hydroxylase and DOPA decarboxylase steps. Once released, dopamine is removed from the synaptic area by dopamine transporters and deactivated by monoamine oxidase and catechol O-methyl transferase. Dopamine acts in the nervous system through G protein-coupled receptors in the presynaptic and postsynaptic sides.

2.7.1 Dopamine receptors

Projections from the substantia nigra pars compacta located in the mesencephalon are responsible for the release of dopamine in the dorsal striatum (Grace, 1991, Bolam et al., 2000). In the striatum, dopamine receptors presynaptically regulate glutamatergic cortico-striatal projections (Bamford et al., 2004b), and postsynaptically modulate the phasic GABAergic firing of spiny projecting neurons (SPNs) (Surmeier et al., 1996).

The class of G protein these receptors are coupled to determines the action of dopamine binding receptors in SPNs. In this manner, dopamine receptors can be classified into D2-like receptor (D2R) – which interacts with G_{i/o} hence decreasing the probability of SPN firing – and D1-like receptor (D1R) – which interacts with G_{s/olf}, hence increasing the firing rate (Surmeier et al., 2007).

The downstream effect of these G proteins can affect glutamate receptor trafficking and the metabolic state of SPNs. Activation of G_s by dopamine D1-like receptor, increases phosphorylation through a cascade that involves adenylyl cyclase activity; therefore, increasing cAMP and protein kinase A. On the contrary, activation of G_i by D2-like receptors decreases phosphorylation through the same cascade but with the opposite effects. This regulation of phosphorylation has related dopamine receptors to the firing probability of SPNs through their action on inward rectifying potassium current channels (Kir K⁺). Kir2-4 K⁺ channels normally hold the membrane potential about -90 mV in typical of SPNs. When they are inactivated by D1-like receptors downstream effects, there is an elevation of the membrane potential that facilitates neuronal firing (Day et al.,

2008), which produces an up state. The action of D2-like receptors prevents this up-state and facilitates a down state by acting on L-type Ca^{2+} (Cav1) and Na^{+} channels (Nav1) that increases hyperpolarization reducing the firing of SPNs (Olson et al., 2005).

The effects of dopamine receptors in glutamate transmission can be presynaptic or postsynaptic. D2-like presynaptic receptors can mediate release of glutamate in corticostriatal projections or affect glutamate receptors activation by dephosphorylation of GluR1 subunits (Hakansson et al., 2006). On the postsynaptic side, dopamine D1-like receptors may generate mobilization of AMPA and NMDA receptors increasing their expression in the synaptic cleft (Hallett et al., 2006). This is accomplished by receptor-receptor interaction, or by striatal-enriched phosphatase, a target of PKA which activates the mobilization of glutamate receptor containing vesicles (Braithwaite et al., 2006). In contrast, the effect of dopamine D2-like receptors on the postsynaptic site decreases glutamate release (Bamford et al., 2004)

2.8 Basal ganglia

The organization of the grey matter in the superficial portion of the brain gives rise to the cortex while in the deep portion is composed of ganglia. These groups of cells are part of the striatum, the thalamus and the mesencephalic ganglia in the cerebrum. The striatum is an important input of cortical signal to the basal ganglia while the thalamus provides input to the cortex and striatum; additionally, the thalamus brings sensory input from the periphery (Bolam et al., 2000). Mesencephalic nuclei provide neuromodulatory input to the cortex, striatum and thalamus regulating their function according to other

organic functions managed in the brain stem like cardiac, respiratory function as well as sleep cycle, eating and the transduction of cranial nerves information. Neurons in the basal ganglia use multiple neurotransmitters to transmit and modulate the signal of the circuit related to the structures they connect.

2.8.1 Striatal circuits

There have been three main striatal pathways described in the literature: The excitatory signal from cortical regions synapses at the caudate nucleus, which may project through GABAergic medium spiny neurons to the globus pallidus internal segment in the direct pathway, or through the globus pallidus external segment in the indirect pathway. This latter pathway inhibits the subthalamic nucleus that in turn excites the globus pallidus; the third one, a more direct pathway projects from the associative cortex directly to the subthalamic nucleus (Nambu et al., 2002). As a consequence, all the output from the striatum to the thalamus integrates in the globus pallidus (Nambu, 2007). This afferent projections from the globus pallidus will inhibit the relay nuclei of the thalamus, which receives them preserving the rostrocaudal topology from the cortex and striatum (Kelly and Strick, 2004). The circuit continues with the excitatory thalamo-cortical projections onto the primary cortex, which closes the loop when inter-cortical connections feedback the associative cortices. In accordance with these circuitries, we hypothesize that the caudal portion of the caudate nucleus could collect projections from associative auditory areas forming an auditory cortico-striatal-thalamo-cortical loop.

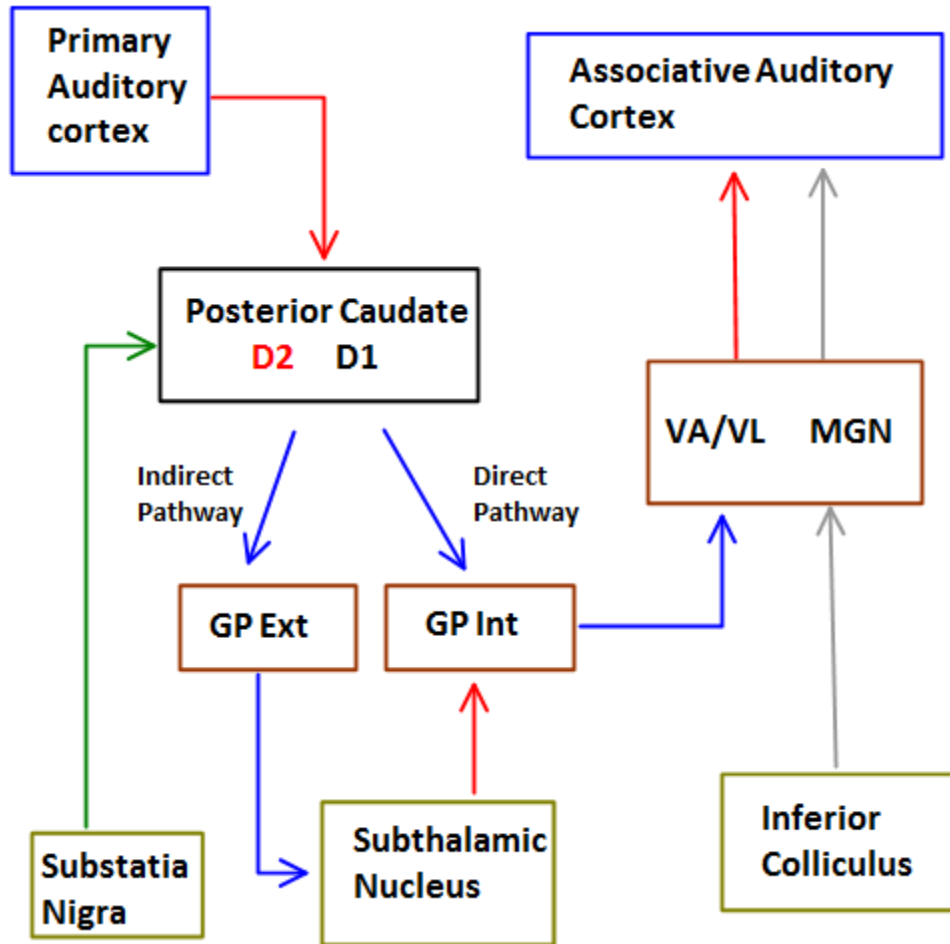


Figure 1. Diagram of the main brain regions related to the auditory cortico-striato-thalamo-cortical circuit. Blue arrows depict GABAergic projections. Red arrows show glutamatergic projections. Green arrow shows dopaminergic projections. Grey arrows correspond to the sensory pathway.

The striatal cytoarchitecture involves the striosome and the matrix compartments. The striosome contains SPNs receive input from the limbic cortex and project to the substantia nigra. The matrix receives input from the cortex and projects to the thalamus through the striatal pathways processing somatosensory and associative signal (Crittenden and Graybiel, 2011).

Abnormal activation of the auditory cortex could arise from an alteration of the striatal pathways, which modulate the signal from primary cortices hence generating a discrepancy in the recurrent cortico efferent feedback (Kelly and Strick, 2004, Happel et al., 2014). The circuits of the basal ganglia regulate neurotransmission of signal from the primary cortices to associative cortices, and so information is computed in order to tune cortical activity at different levels of the striatum (Graybiel, 1997).

Dopaminergic projections modulate the striatal pathways, a useful process that helps us interpret dysconnectivity among circuits as a pathophysiological mechanism that generates schizophrenia-like symptoms (Stephan et al., 2009). These SPNs projections synapse neurons in the interface nuclei via two canonical pathways: (a) an indirect pathway that first synapse at the globus pallidus external segment and then loops through the subthalamic nucleus, and (b) a direct pathway that synapses primarily with the interface nuclei constituted by the globus pallidus internal segment and the substantia nigra pars reticulata (Nambu, 2007).

SPNs of the indirect pathway predominantly express D2R while SPNs of the direct pathway express D1R (Gerfen et al., 1990, Gong et al., 2003). Consequently, DA release in the striatum decreases the output from the interface nuclei to the thalamus by favoring a down state in the D2R expressing SPNs of the indirect pathway, or alternatively increases the output from globus pallidus by activating D1R expressing SPNs firing in the direct pathway (Gerfen and Surmeier, 2011a). The GABAergic projections of the globus pallidus in turn disinhibit thalamic activity and allow the glutamatergic thalamic

output to the cortex and striatum to increase providing positive feedback to the cortico-striato-thalamo-cortical circuits (Figure 1).

The striatal circuits have been mapped with viral vectors showing the topography preserved through the pathways (Kelly and Strick, 2004). The head of the caudate receives connection from the frontal cortex and motor cortex, while more ventral areas connect with the limbic system. In this way, the posterior and narrow portion of the striatum has afferent connections from the parietal and sensory cortices (Kimura et al., 2004). In these neuroanatomical studies, the circuits that interact with the cortex have shown close and open loops (Kelly and Strick, 2004). These refer to connection that can provide feedback to their cortical origin or that provide input to a different cortical region.

In the case of the motor system, for example, the striatal pathways promote movement through the direct pathway or inhibit movement through the indirect pathway (Bateup et al., 2010). Interconnections between the striatal pathways provide fine modulation of these circuits to select the appropriate the motor pattern. However, the sophisticated role of the striatal pathways in filtering and tuning the cortical function requires both direct and indirect interaction of circuits (Calabresi et al., 2014).

2.9 Mechanism for intrinsic auditory activation

The cells in the striatal pathways work as autonomous pacemakers, which fire spontaneously following fluctuations in the resting membrane potential. This activity can be modulated by neurotransmitters like dopamine. Recurrent efferent cortical projections

provide a feed forward mechanism that may activate cortical networks (Happel et al., 2014) especially when considering the pacemaker characteristics of the striatal neurons.

Corticostriatal inputs has been characterized into two groups: the inter-telencephalic tract and the pyramidal tract (Shepherd, 2013). These projections preserve their topography on their target regions; hence, they differ in their connectivity to the striosome and matrix (Crittenden and Graybiel, 2011). These spiny projecting cells receive an efferent copy of cortical activity and primarily synapse in D2R expressing cells (Lei et al., 2004). Thus, imbalances in recurrent circuits with positive feedback onto cortical activity may produce intrinsic activation of cortex through striatal networks.

The effects of dopamine in postsynaptic D2-like receptors on corticostriatal circuits may produce enhance cortical auditory activity. A supersensitive D2-like receptor would silence the activity of spiny projecting neurons, which in the indirect striatal pathway disinhibit GABAergic release by the globus pallidus into the thalamus; therefore, it would produce increased output in thalamo-cortical projections.

The posterior portion of the caudatoputamen receives projections from the auditory cortex (Kimura et al., 2004). Due to the preserved anatomical topography of these cortical efferent projections throughout their circuits, these subcortical targets project back to cortical regions with parallel function; in this case, the posterior caudatoputamen would project back to the auditory and parietal cortices. As a result, were the mechanism of cortical activation by supersensitive D2-like receptor present in the posterior caudatoputamen, it might give rise to enhance auditory activation.

CHAPTER 3

DOPAMINE-INDUCED AUDITORY CORTICAL ACTIVATION AND ATTENUATION BY D₂-LIKE RECEPTOR-SELECTIVE ANTAGONIST IN THE CAUDATOPUTAMEN OF THE RAT

3.1 Project Summary

Background: The metabolism of auditory cortex increases during auditory hallucinations. These phenomena are a characteristic symptom of schizophrenia. Dopamine D₂-like receptor antagonists are used to treat schizophrenia, and neuromodulatory effects of dopamine in the basal ganglia are central to the neuropathology of schizophrenia. However, the mechanisms by which DA dysfunction produces symptoms of schizophrenia are not understood.

Methods: We evaluated the effect of unilateral DA infusion (0, 12.5, 25 and 50 nM in 0.5 µl saline vehicle), or DA co-infusion with 20 nM eticlopride, a dopamine D₂-like receptor selective antagonist, into caudal caudatoputamen (-1.8 mm from bregma) on functional activity in auditory cortex of rats. Expression of the immediate early gene, *zif268* mRNA was quantified using *in situ* hybridization histochemistry as a measure of functional activation. The effects of sound (15 dB over ambient) and light exposure on *zif268* mRNA were also examined.

Results: Striatal dopamine infusion caused a dose-dependent increase of *zif268* mRNA expression in the auditory cortex, with 50 µM dopamine producing *zif268* mRNA

expression similar to that produced by sound. These cortical effects were highly localized with a distinct laminar pattern. Eticlopride co-infusion attenuated the functional activation induced by 50 μ M dopamine alone.

Conclusion: These data are consistent with participation of striatal dopamine in the activation of auditory cortex. The regional and laminar localization of this effect suggests that perception of sound may be present. The attenuation achieved by dopamine D₂-like receptor antagonism is consistent with the therapeutic effect of antipsychotics. We propose this paradigm as a model of endogenous auditory activation that may elucidate the biological bases of psychotic symptoms.

3.2 Introduction

Total costs related to schizophrenia are estimated to be \$65 billion per year in the U.S. alone (Davies and Drummond, 1994, Knapp et al., 2004). With a prevalence of one percent and an onset in early adulthood, the occurrence of this disease has life-long repercussions and a poor prognosis (E, 1971, Freedman, 2003). Perturbations of mental functions such as flattened affect, anhedonia and impoverished speech contrast with symptoms such as hallucinations and delusions within the clinical framework of schizophrenia (Tandon et al., 2013). These manifestations suggest an imbalance of multiple circuits and the involvement of various brain regions (Stephan et al., 2009). A cardinal symptom characterizing schizophrenia is auditory hallucinations (Battle, 2013), wherein increased metabolic activity of the temporal cortex arises from aberrant activation (Bentaleb et al., 2002). Excessive dopamine (DA) has been detected in the

striatum of patients with schizophrenia (Abi-Dargham et al., 1998), and the affinity of antipsychotic drugs for D₂-like DA receptors (D₂R) correlates with their ability to alleviate positive symptoms, including auditory hallucinations (Seeman and Guan, 2008, Johnsen et al., 2013, Madras, 2013). In fact, neurons of auditory association cortex in the rat project directly to a posterior region of the caudatoputamen (Gangarossa et al., 2013). However, much less is known about the putative neuronal mechanisms that link striatal DA transmission to activation of the auditory cortex.

Auditory stimuli normally achieve cortical awareness after relay with neurons in the medial geniculate nucleus of the thalamus, whose projections terminate in layer IV of primary auditory cortex. The present study evaluated the effect of tonal stimulus 15 dB above ambient level on functional activation in the various cortical layers of regions within and surrounding auditory cortex. The effect of the tonal stimulus was compared to that produced by a DA injection into the region of the posterior caudatoputamen that is innervated by auditory association cortex (Kimura et al.), as well as that produced by a light stimulus. We also evaluated the effect of a selective D₂R antagonist co-infused with DA on the functional activity of the auditory cortex. Functional activation was measured by expression of the immediate early gene, *zif268*, which is rapidly affected by natural synaptic activity, particularly in cerebral cortex (Worley et al., 1991). This functional marker is constitutively expressed, which allows us to assess bidirectional changes in neuronal activity.

We hypothesize that enhanced DA signaling in the posterior caudatoputamen induces selective functional activation of auditory cortex in a manner similar to that produced by

sound, and that this cortical activation will be blocked by a D₂R antagonist; if so, this could demonstrate an endogenous brain mechanism to activate the primary auditory cortex. We believe these findings are important to better understand the pathophysiology of schizophrenia-like symptoms.

3.3 Experimental Design

Subjects: Eighty-one adult male Sprague Dawley rats weighing 250 g from Charles River Laboratories were group-housed in a temperature- and humidity-controlled room, and were habituated to a reverse light/dark cycle (lights on from 1900 to 0900 h) for 5 days with food and water available *ad lib*. All experiments were approved by the University of Arizona and Arizona State University Institutional Animal Care and Use Committee in accordance to the Guide for the Care and Use of Laboratory Animals.

Drugs: Dopamine HCl (Patterson Veterinary Supply; Phoenix, AZ) was diluted with 0.9% sterile saline vehicle to 12.5, 25, 50 and 100 nM solutions. Eticlopride HCl (Tocris Bioscience; Minneapolis, MN) was reconstituted with 0.9% sterile saline vehicle to 40 nM, then infused with an equal volume of 100 nM DA for final concentrations of 50 nM DA and 20 nM eticlopride.

Cannula implantation: Rats were anesthetized with isoflurane and were mounted in a stereotaxic frame. Unilateral infusion cannulas targeting the posterior caudatoputamen (AP: -1.8 mm, ML: -4.5 mm, and DV: 6.0 mm; Paxinos and Watson, 2007) were surgically implanted and fixed to the skull. Rats were then allowed to recover for seven days.

3.3.1 Striatal dopamine dose dependent study

We conducted this study with nine rats per treatment group. Rats were randomly assigned to one of five treatment groups, which received intracranial infusion of either saline vehicle or 12.5, 25 or 50 nM DA with 70 dB ambient sound in a dark chamber, or saline vehicle with 85 dB sound in a dark chamber.

3.3.2 Laminar assessment of the auditory cortex

In this study, we replicate some of the previous treatments and add a light stimulus to assess the specificity of the effect in the auditory cortex. Thus, nine animals per group were randomly assigned to four treatment groups. Three groups received an intracranial infusion of saline vehicle and one group 50 nM of dopamine. In the saline vehicle groups one received a sound stimulus of 85 dB while the rest had an ambient noise of 70 dB, and another group had the light on while the rest had a dark chamber.

3.3.3 Co-infusion of dopamine antagonists and dopamine in the striatum

In the following study, four additional groups were randomly assigned to receive infusion of saline vehicle, 50 nM DA, 20 nM eticlopride, or 50 nM DA/20 nM eticlopride co-infusion, each with 70 dB ambient sound.

Intracranial infusions (volume: 0.50 μ l; infusion rate: 0.25 μ l/min; infusion cannula remained in place for 5 min, then was slowly withdrawn) were performed, then rats were transferred to a sound-attenuated chamber (10" W X 8" D X 10" H) for one hour with the appropriate sound level. Immediately following the sound session, rats were anesthetized

and perfused with ice-cold 4% buffered paraformaldehyde, and brains were removed, post-fixed placed in graded sucrose solutions for 48 h, then stored at -80°C prior to processing.

3.3.4 *Zif268* probe labeling

An oligodeoxyribonucleotide probe whose sequence is complementary to amino acids 2-16 of the *Zif268* protein (5'CCGTTGCTGAGCATCATCTCCTCCAGTTTGGGGTAGTTGTCC3') was 3' end-labeled with [³⁵S]dATP (PerkinElmer; Waltham, MA) using terminal deoxynucleotidyl transferase (New England Biolabs; Ipswich, MA), as described previously (Hammer and Cooke, 1996). This probe has been characterized by the research group in Graybiel's laboratory where the sense and missense probe were tested for control expression and equivalent standards obtained for the quantification of mCi/mg of tissue (Moratalla et al., 1992). The implementation of *zif268* in the study of dopamine induced metabolic changes in brain slices have been previously reported (Keefe and Gerfen, 1996). Briefly, the probe was purified and diluted with hybridization buffer containing 50% formamide, 500 µg/ml sheared salmon sperm DNA, 250 µg/ml yeast tRNA, 4 × saline-sodium citrate (SSC), 1 × Denhardt's solution, and 10% dextran sulfate/dithiothreitol solution to yield a 3 × 10⁷ dpm/ml of hybridization solution.

3.3.5 Tissue preparation and *in situ* hybridization histochemistry (ISHH)

Brains were cryosectioned at 20 µm and sections were collected at -3.6 mm to -4.5 mm from bregma (Paxinos and Watson, 2007), and thaw-mounted on microslides.

Infusion sites were confirmed, and slides were prepared for ISHH (Covington et al., 2005). Briefly, slides were postfixed in 10% formaldehyde in 10 mM phosphate buffered saline, pH 7.4 (PBS) for 10 min, rinsed and acetylated in 0.25% acetic anhydride in 0.9% NaCl/0.1 M triethanolamide, pH 8.0 (TEA) for 10 min, then dehydrated, delipidated, and air-dried. Slides were placed into humidified RNase-free chambers, covered with hybridization solution under Parafilm® coverslips overnight at 37°C. Coverslips were removed and slides were washed at 23°C in 0.3 M NaCl sodium 30 nM sodium citrate, pH 7.0 (2× SSC) and 50% formamide for 1 h, twice in 1× SSC and once in 0.5× SSC for 30 min each, then washed in 0.1 SSC at 37 °C for 30 min. The tissue was washed twice in 1 × SSC for 30 min, and dehydrated in graded ethanol solutions before being air-dried. Hybridized slides were randomized and exposed to Biomax-MR X-ray film (Carestream Health) co-exposed with calibrated radiostandards (American Radiolabeled Chemicals; St. Louis, MO) which had been cross-calibrated to ³⁵S-brain paste standards (Hammer, Bogic and Handa, 1993); films were developed using a table-top processor (Konica Minolta, SRX-101A).

3.3.6 Image analysis

Films were scanned for densitometric analysis using ImageJ analysis software (created by Wayne Rasband; available at: <http://rsb.info.nih.gov/ij/>). Each film had a radio standard for calibration of the respective slides. Slides were stained with cresyl violet stain and scanned to permit precise localization of brain regions. Thus, the agranular motor cortex was differentiated from the granular auditory and the visual cortex. Due to the intersperse distribution of layer IV on the rostrocaudal access

distinction of the surrounded secondary sensory cortex was not carried out. Then, high resolution scans of autoradiographs and stained sections were aligned using TurboReg image registration plug-in (created by Philippe Thévenaz; available at: <http://bigwww.epfl.ch/thevenaz/turboreg/>). Following calibration using autoradiographic images of the radiostandards, anatomical regions of interest were outlined on the stained section and *zif268* mRNA was quantified on film images in terms of mCi/mg tissue protein. The depth of each layer was recorded in pixels and the distance then calculated as a factor of 2.6 μm per pixel. To facilitate comparisons between layers in our model each layer was then consider as a percentage of total cortical depth. In this manner, in the auditory cortex Layer II: 11%, Layer III: 12%, Layer IV: 22%, Layer V: 25% and Layer VI: 30%. In the motor cortex Layer II: 14%, Layer III: 34%, Layer IV: 0%, Layer V: 63% and in the visual cortex Layer II: 14%, Layer III: 26%, Layer IV: 47%, Layer V: 74%.

3.3.7 Statistical analyses

ANOVAs were performed to determine treatment effects using the following planned comparisons: (a) difference in mean expression of *zif268* between ipsilateral and contralateral auditory cortices, (b) differences between doses of dopamine, (c) differences between cortical layers along rostro-caudal levels of the auditory cortex, (d) differences between co-infused eticlopride and all other dopamine groups. (e) differences between auditory, motor and visual cortices. Specific effects were evaluated considering Bonferroni's adjustment for multiple comparisons.

Figure 2. Target region and injection sites recorded for intracranial injections of dopamine doses and saline vehicle.

3.4.2 Sound and DA dose dependently increase expression of *zif268* mRNA in auditory cortex

We quantified the expression of *zif268* mRNA across all layers of auditory cortex from rats held within a sound attenuated chamber at ambient sound levels of 70 and 85 dB (Figure 3A). The 85 dB stimulus significantly increased functional activation of the entire auditory cortex compared to 70 dB ambient sound ($\Delta = 0.444$, $t = 4.95$, $p \leq 0.0001$). Therefore, 70 dB sound was utilized as the background sound in all subsequent infusion experiments.

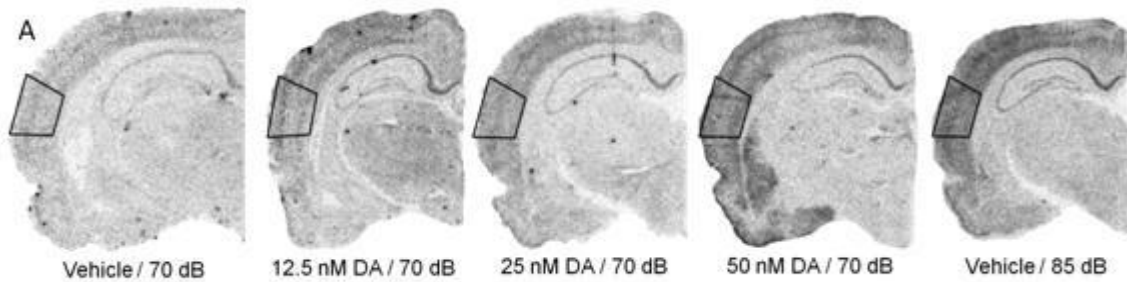


Figure 3. Effects of 12.5 nM, 25 nM and 50 nM of DA infusion and 85 dB sound stimulus in the caudal caudatoputamen on the expression of *zif268* mRNA in auditory cortex.

Figure 3A. Each hemisection corresponds to an example of a treatment group. Autoradiography of *zif268* mRNA at -4.3 mm from bregma. The delineated area of the temporal cortex corresponds to the quantified auditory region.

We then examined functional activation of auditory cortex following infusion of 0, 12.5, 25, or 50 nM doses of DA, and compared the DA effects to those produced by ambient sound levels of 70 or 85 dB (Figure 3B & Table 1). Infusion of 12.5 nM of DA significantly increased *zif268* mRNA expression in the auditory cortex (12.5 nM DA vs. vehicle $\Delta = 0.187$, $t = 2.08$, $p \leq 0.05$). A 25 nM injection of DA produced similar expression of *zif268* mRNA in the auditory cortex to the 12.5 nM DA injection, and significantly higher than vehicle (25 nM DA vs. vehicle $\Delta = 0.224$, $t = 2.50$, $p \leq 0.05$). Subsequently, the increase from 25 nM to 50 nM of DA augmented the expression of *zif268* mRNA up to an equivalent activation generated by a sound 15 dB higher than ambient noise (50 nM DA vs. vehicle $\Delta = 0.484$, $t = 5.69$, $p < 0.001$) (Figure 3B).

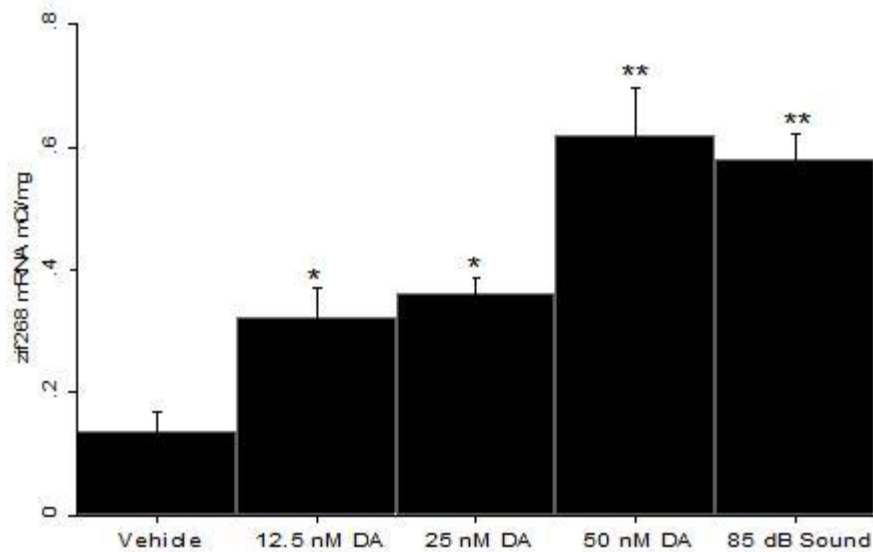


Figure 3B. Mean expression of the *zif268* mRNA in the auditory cortex after incremental doses of DA. There is a dose dependent effect with increased dose of DA (ANOVA

$F_{(4,24)}: 10.48$, $p < 0.00001$).

Auditory Cortex		
	0.0000	
	Vehicle	85 dB Sound
85 dB Sound	0.000	
50 nM DA	0.000	0.681
25 nM DA	0.050	0.037
12.5 nM DA	0.048	0.042

Table 1. P values of planned comparisons of the *zif268* mRNA expression after DA injection in the posterior caudate.

Interestingly, comparison of functional activation between hemispheres revealed no significant differences in response to any DA dose (12.5 nM Right vs. Left $F_{(1,8)}$: 0.03, $p > 0.05$; 25 nM Right vs. Left $F_{(1,10)}$: 0.26, $p > 0.05$; 50 nM Right vs. Left $F_{(1,8)}$: 3.37, $p > 0.05$) (Figure 3C).

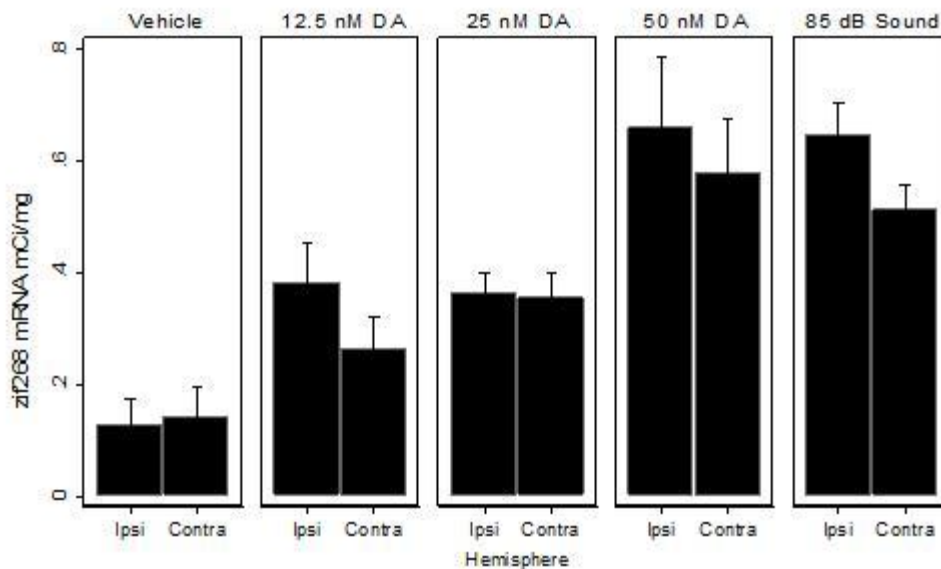


Figure 3C. Inter-hemispheric comparison of *zif268* mRNA expression in the auditory cortex. No significant differences were detected in the expression of *zif268* mRNA when comparing the two hemispheres.

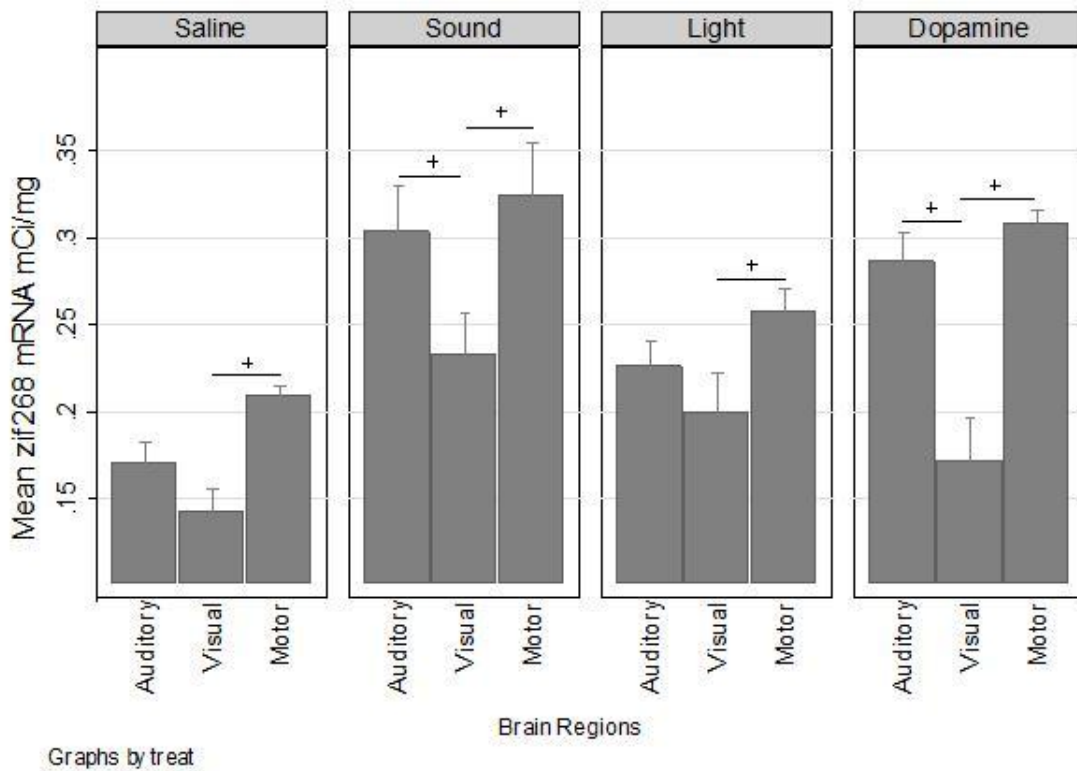


Figure 4. Functional activation by sound, dopamine, light and saline treatments in the cortical layers of the auditory, visual and motor cortices. Mean *zif268* mRNA expression shown in the Y axis for every treatment across the cortical regions evaluated. Error bars depict one standard error of the mean.

Treatments	Saline 0.0173		Sound 0.0398		Light 0.0237		Dopamine 0.0000	
	Auditory	Visual	Auditory	Visual	Auditory	Visual	Auditory	Visual
Visual	0.924		0.290		0.784		0.002	
Motor	0.481	0.014	1.000	0.046	0.605	0.020	1.000	0.000

Table 2. P-values of ANOVA and Bonferroni's test hypothesizing equal functional activation in auditory, visual and motor regions.

Note 1: Table reports the p-values of the F-statistic for ANOVA testing the hypothesis of equal mean *zif268* mRNA expression between brain regions by treatment (top region of the table). Planned comparisons using Bonferroni's adjusted F-statistic were carried out subsequently to detect specific regional differences (Bottom region of the table). Refer to Annex 2 for details of each test.

After a comparison of treatment effects between regions, saline treatment showed low levels of *zif268* mRNA expression in all brain regions. The motor region, however, exhibits higher functional activation compared to the auditory and visual regions. This was observed in all treatments including saline. Such effect could be explained by deambulation of the animals in the sound insulated chamber, though the higher constitutive expression levels in the motor cortex may mask its assessment as control region for sensory brain areas. Moreover, the light treatment showed unexpected low activation of the visual cortex. In fact, the visual region showed the lowest functional activation in all treatments. The effects of sound and dopamine treatments did replicated our previous findings inducing higher functional activation, especially in the auditory and

motor regions. These mean expression levels were followed up with post-hoc testing to identify differences between cortical layers.

Saline	Layer II 0.0941		Layer III 0.2370		Layer IV 0.5653		Layer V 0.0805		Layer VI 0.0522	
	Obs	Rank Sum	Obs	Rank Sum	Obs	Rank Sum	Obs	Rank Sum	Obs	Rank Sum
Auditory	7	70	7	71	7	57	7	75	6	73
Visual	7	56	7	61	7	48	7	52	6	51
Motor	7	105	7	99	.	.	7	104	5	107

Sound	Layer II 0.0813		Layer III 0.3102		Layer IV 0.2002		Layer V 0.3551		Layer VI 0.8712	
	Obs	Rank Sum	Obs	Rank Sum	Obs	Rank Sum	Obs	Rank Sum	Obs	Rank Sum
Auditory	7	62	6	60	6	47	6	54	6	59
Visual	7	32	6	39	6	31	6	42	6	50
Motor	7	58	5	54	.	.	5	57	5	44

Light	Layer II 0.0444		Layer III 0.1837		Layer IV 0.3865		Layer V 0.1532		Layer VI 0.4152	
	Obs	Rank Sum	Obs	Rank Sum	Obs	Rank Sum	Obs	Rank Sum	Obs	Rank Sum
Auditory	9	122	9	128	9	90	9	118	9	116
Visual	8	65	8	73	8	63	8	75	8	85
Motor	8	138	8	124	.	.	8	132	8	124

Dopamine	Layer II 0.0157		Layer III 0.0075		Layer IV 0.0283		Layer V 0.0240		Layer VI 0.0455	
	Obs	Rank Sum	Obs	Rank Sum	Obs	Rank Sum	Obs	Rank Sum	Obs	Rank Sum
Auditory	5	51	5	48	5	38	5	44	5	47
Visual	5	25	5	15	5	17	5	19	5	20
Motor	5	60	5	57	.	.	5	57	5	53

Table 3. P-values of Kruskal-Wallis test hypothesizing similar functional activation in brain regions by cortical layers

Note 1: Cortical Layer II (Cortical depth $\leq 11\%$), Layer III ($11\% < \text{depth} \leq 23\%$), Layer IV ($23\% < \text{depth} \leq 45\%$), Layer V ($45\% < \text{depth} \leq 70\%$), Layer VI ($70\% < \text{depth} \leq 100\%$).

Saline: control treatment to Sound, Light and Dopamine. Light: control modality

treatment to Sound. Dopamine: hypothesis treatment. Motor (-3.8 mm from bregma):

Control brain region to Auditory and Visual. Visual (-5.8 mm from bregma): Control modality region to Auditory.

Note 2: Tables report the p-values of the Kruskal-Wallis test hypothesizing equal *zif268* mRNA expression between brain regions at each cortical layer (Top region of each table). The number of brains per region is listed under the column Obs. The rank of the region within each layer per treatment is listed under Rank Sum. Refer to Annex 2 for detail of each test.

At the laminar level, each brain region has a distinctive cytoarchitecture. The most predominant factor is the well-differentiated layer IV in sensory cortices, which is almost absent in the motor cortex. Therefore, a non-parametric analysis allowed between regions laminar comparisons without violating the normality and equal variances assumptions for ANOVA. A Kruskal-Wallis test was performed to test if the *zif268* mRNA expression was similar between auditory, visual and motor regions at each cortical layer.

Dopamine treatment induced a higher expression of *zif268* mRNA in all layers of the motor cortex compared to the sensory regions. In the sensory regions, dopamine induced higher functional activation in layer IV of the auditory cortex compared to the same layer in the visual cortex. This effect in the input layer of sensory regions was not statistically differentiable in sound or light treatment groups. Other treatments did not report significant laminar differences between regions, except for the layer II after light treatment. In spite of the low effect by light in the visual cortex, the predominant effect of

dopamine in the auditory cortex indicated that a more detailed evaluation of within each brain region was necessary.

Laminar analysis: The response in each layer of auditory cortex to 50 nM striatal DA infusion was then compared across rostro-caudal levels from bregma -3.8 mm to -5.2 mm (Paxinos and Watson, 2007) (Figure 5), which revealed a significant main effect of level ($F_{(4,24)}: 10.48, p \leq 0.00001$). Dopamine-induced functional activation was greater -4.4 mm from bregma (ANOVA: level -4.4 mm $F_{(3,23)}: 4.06, p \leq 0.05$). Dopamine showed a lesser effect on *zif268* mRNA expression at -4.0 mm level with intermediate readings at -3.8 mm and -4.2 mm levels. By contrast, striatal DA infusion had no effect on *zif268* mRNA expression in agranular motor cortex ($F_{(4,38)}: 0.75, p > 0.05$). Laminar analysis of cortex conducted across the same rostro-caudal levels revealed that 85 dB sound significantly increased *zif268* mRNA expression in layers III and IV at -3.8 mm, and in all layers at -4.0, -4.8 and -5.2 mm from bregma compared to the saline group (Table 2). Even though the effect of light treatment can be statistically differentiated from sound treatment in layers II-IV at -4.0 mm from bregma, light treatment was not statistically significant different from control group in any other rostrocaudal level.

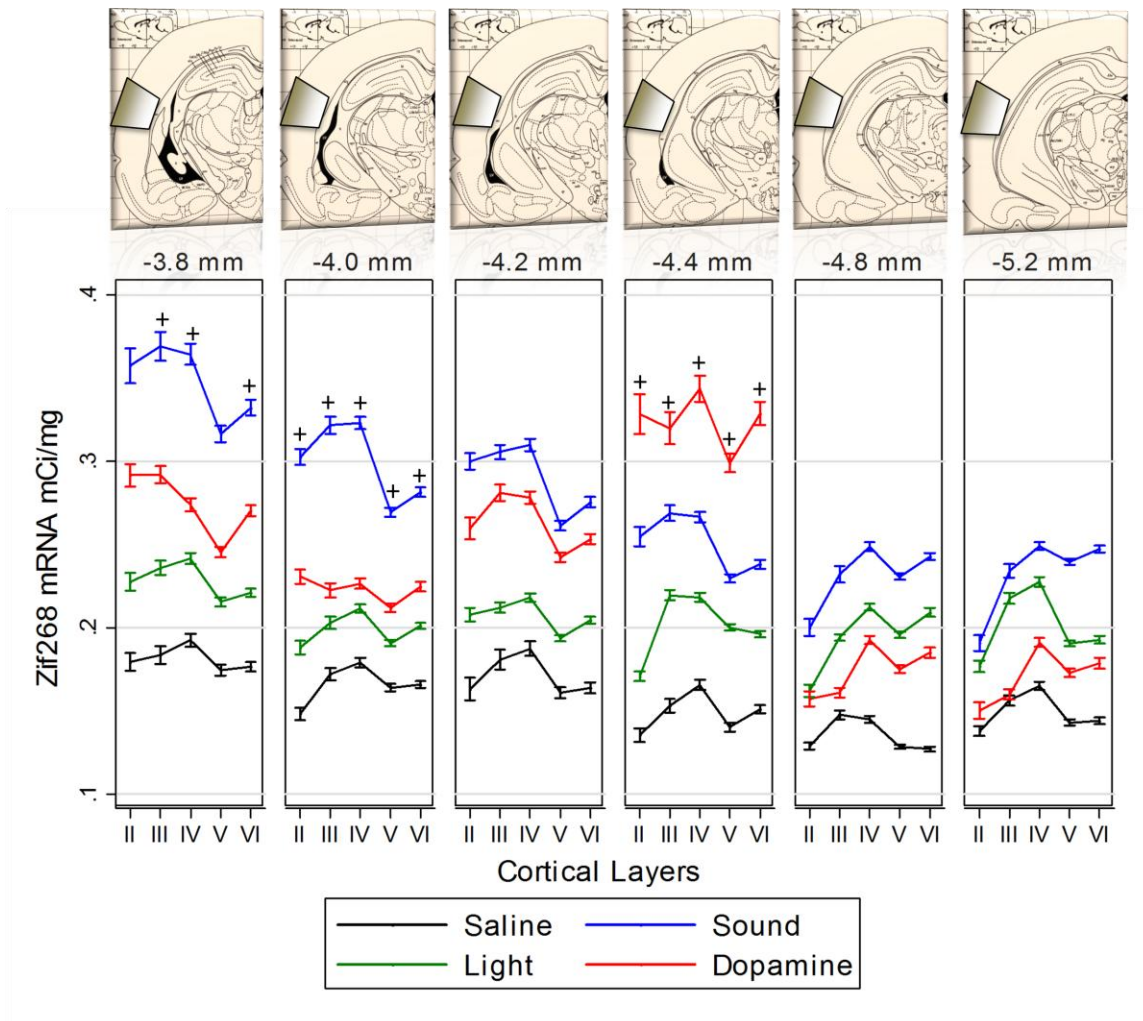


Figure 5. Functional activation of the auditory cortex by sound, dopamine, light and saline treatments in cortical layers at six rostrocaudal levels. Mean expression of *zif268* mRNA from -3.8 mm to -5.2 mm levels of the temporal cortex across cortical depth for each treatment group.

Black: Saline intracranial injection (Control group); Blue: 85 dB sound stimulus group (Modality specific treatment); Green: Light group (Modality control treatment); Red: Dopamine group (Modality hypothesis treatment). Error bars depict one standard error around the mean. Plus signs on top of error bars depict significant difference between

treatments within a cortical layer. On the rostrocaudal axis, each level has a different input profile: At -3.8 mm from bregma all treatment groups differ in the expression level of *zif268* mRNA with sound producing a higher effect. At -4.0 mm from bregma, sound treatment generates activation while other treatments show low activation levels. The posterior levels (-4.2 mm and -4.4 mm) do not exhibit sound induced activation while dopamine treatment activates the auditory cortex at -4.4 mm and other treatments show low *zif268* mRNA expression.

-3.8 mm	Layer II 0.0704		Layer III 0.0312		Layer IV 0.0576		Layer V 0.0666		Layer VI 0.0376	
Sound	Saline 0.088	Sound 1.000	Saline 0.032	Sound 0.176	Saline 0.054	Sound 0.263	Saline 0.066	Sound 0.295	Saline 0.041	Sound 0.207
Light	1.000	0.318	1.000	0.176	1.000	0.263	1.000	0.295	1.000	0.207
Dopamine	0.682	1.000	0.510	1.000	1.000	1.000	1.000	1.000	0.513	1.000
-4.0 mm	Layer II 0.0029		Layer III 0.0086		Layer IV 0.0077		Layer V 0.0224		Layer VI 0.0285	
Sound	Saline 0.002	Sound 1.000	Saline 0.008	Sound 0.031	Saline 0.007	Sound 0.033	Saline 0.019	Sound 0.100	Saline 0.024	Sound 0.154
Light	1.000	0.021	1.000	0.031	1.000	0.033	1.000	0.100	1.000	0.154
Dopamine	0.292	0.537	1.000	0.226	1.000	0.176	1.000	0.643	0.877	0.909
-4.2 mm	Layer II 0.0931		Layer III 0.0463		Layer IV 0.0860		Layer V 0.0573		Layer VI 0.0727	
Sound	Saline 0.119	Sound 1.000	Saline 0.091	Sound 0.257	Saline 0.146	Sound 0.357	Saline 0.089	Sound 0.391	Saline 0.103	Sound 0.534
Light	1.000	0.449	1.000	0.257	1.000	0.357	1.000	0.391	1.000	0.534
Dopamine	0.703	1.000	0.314	1.000	0.597	1.000	0.339	1.000	0.388	1.000
-4.4 mm	Layer II 0.0138		Layer III 0.0259		Layer IV 0.0291		Layer V 0.0146		Layer VI 0.0211	
Sound	Saline 0.276	Sound 0.826	Saline 0.189	Sound 1.000	Saline 0.459	Sound 1.000	Saline 0.298	Sound 1.000	Saline 0.627	Sound 1.000
Light	1.000	0.826	0.986	1.000	1.000	1.000	0.814	1.000	1.000	1.000
Dopamine	0.020	1.000	0.028	1.000	0.027	1.000	0.011	0.865	0.018	0.680
-4.8 mm	Layer II 0.0867		Layer III 0.0081		Layer IV 0.0010		Layer V 0.0013		Layer VI 0.0025	
Sound	Saline 0.094	Sound 0.969	Saline 0.009	Sound 0.642	Saline 0.001	Sound 0.750	Saline 0.001	Sound 0.892	Saline 0.002	Sound 1.000
Light	1.000	0.969	0.264	0.642	0.017	0.750	0.018	0.892	0.019	1.000
Dopamine	1.000	0.357	1.000	0.059	0.272	0.214	0.300	0.242	0.245	0.550

-5.8 mm	Layer II		Layer III		Layer IV		Layer V		Layer VI	
	0.2447		0.0124		0.0377		0.0033		0.0079	
	Saline	Sound	Saline	Sound	Saline	Sound	Saline	Sound	Saline	Sound
Sound	0.424		0.039		0.053		0.002		0.005	
Light	0.978	1.000	0.122	1.000	0.176	1.000	0.180	0.266	0.314	0.327
Dopamine	1.000	1.000	1.000	0.087	1.000	0.504	1.000	0.091	1.000	0.211

Table 4. P values of MANOVA and Bonferroni's adjusted F-statistic hypothesizing similar functional activation in layers of the temporal cortex by treatments at each rostrocaudal level.

Note 1: Cortical Layer II (Cortical depth $\leq 11\%$), Layer III ($11\% < \text{depth} \leq 23\%$), Layer IV ($23\% < \text{depth} \leq 45\%$), Layer V ($45\% < \text{depth} \leq 70\%$), Layer VI ($70\% < \text{depth} \leq 100\%$).

Saline: control treatment to Sound, Light, and Dopamine. Light: control modality treatment to Sound. Dopamine: hypothesis treatment.

Note 2: Tables report the p-values of the F-statistic for MANOVA testing the hypothesis of equal mean *zif268* mRNA expression between treatment groups at each rostrocaudal level (top panel on each table). Planned comparisons using Bonferroni's adjusted F-statistic were carried out subsequently to detect specific treatment effects per layer (bottom panel on each table). Highlighted values depict statistical significance achieved. Refer to Appendix 2 for details on each test.

-3.6 mm	Layer II		Layer III		Layer V		Layer VI	
	0.2726		0.2578		0.3613		0.4271	
	Saline	Sound	Saline	Sound	Saline	Sound	Saline	Sound
Sound	0.535		0.002		1.000		1.000	
Light	1.000	1.000	0.180	0.266	1.000	1.000	1.000	1.000
Dopamine	0.681	1.000	1.000	0.091	0.719	1.000	0.771	1.000

-3.8 mm	Layer II		Layer III		Layer V		Layer VI	
	0.0423		0.0453		0.0759		0.1742	
	Saline	Sound	Saline	Sound	Saline	Sound	Saline	Sound
Sound	0.038		0.044		0.088		0.256	
Light	1.000	0.290	1.000	0.487	1.000	0.600	1.000	1.000
Dopamine	0.599	1.000	0.396	1.000	0.484	1.000	0.665	1.000

Table 5. P-values of MANOVA and Bonferroni's adjusted F-statistic hypothesizing similar functional activation in layers of the motor cortex by treatments at each rostrocaudal level.

Note 1: Cortical Layer II (Cortical depth $\leq 11\%$), Layer III ($11\% < \text{depth} \leq 23\%$), Layer IV ($23\% < \text{depth} \leq 45\%$), Layer V ($45\% < \text{depth} \leq 70\%$), Layer VI ($70\% < \text{depth} \leq 100\%$).

Saline: control treatment to Sound, Light and Dopamine. Light: control modality treatment to Sound. Dopamine: hypothesis treatment.

Note 2: Tables report the p-values of the F-statistic for MANOVA testing the hypothesis of equal mean *zif268* mRNA expression between treatment groups at each rostrocaudal level (top region on each table). Planned comparisons using Bonferroni's adjusted F-statistic were carried out subsequently to detect specific treatment effects per layer (Bottom region on each table). Refer to Annex 4 for details of each test.

The effects of sound were significantly greater in layers II and III at -3.8 mm from bregma. Dopamine and sound treatments induced a mean expression of *zif268* mRNA up

to 0.35 mCi/mg in level -3.6 mm. Although there were no differences between the effects of other treatments, it is important to mention that all treatments including saline showed higher functional activation.

3.4.3 Dopamine selective antagonist attenuate dopamine induce auditory activation

Eticlopride was co-infused with DA in order to avoid non-specific effects of D₂R blockade in other brain regions. Compared to infusion of DA alone, co-infusion in the posterior caudatoputamen significantly reduced expression of *zif268* mRNA in auditory cortex ($F_{(1,39)}: 8.836, p \leq 0.005$), to a level that did not differ from that produced by infusion of vehicle (Fig. 3). Eticlopride alone did not alter *zif268* mRNA expression in auditory cortex compared to vehicle treatment ($F_{(1,39)}: 1.084, p = 0.305$), nor did co-infusion or eticlopride infusion affect functional activation in agranular motor cortex ($F_{(5,39)}: 0.609, p = 0.69$).

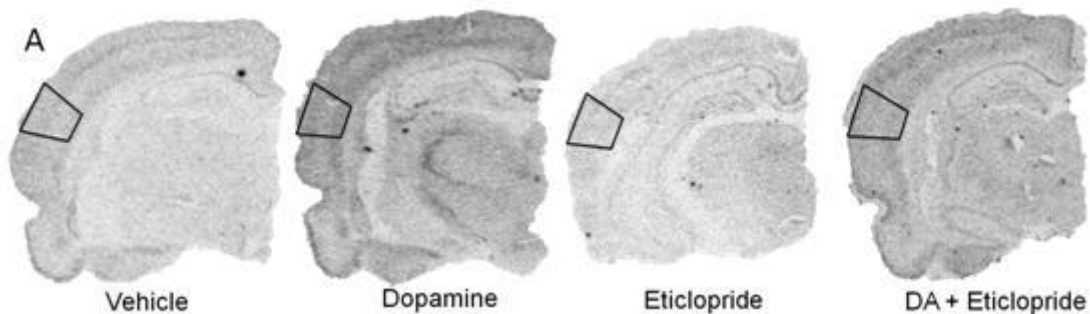


Figure 6. D₂-like selective antagonist attenuates DA-induced functional activation of auditory cortex.

Figure 6A. Each hemisection corresponds to an example from each treatment group.
Autoradiography of *zif268* mRNA at the auditory cortex.

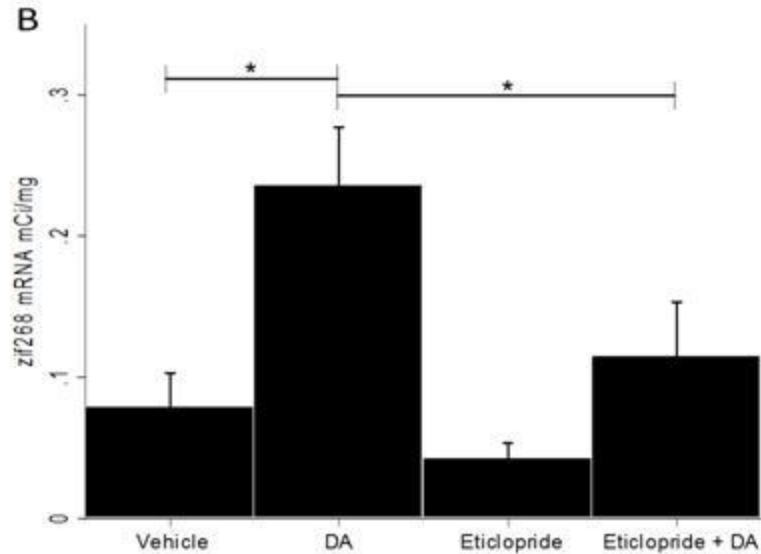


Figure 6B. Mean expression of *zif268* mRNA in auditory cortex after injection of 50 nM of DA, 20 nM of eticlopride or coinfusion of 50 nM of DA + 20 nM of eticlopride. * indicates statistically significant comparisons. DA: 50 nM DA increased *zif268* mRNA expression in auditory cortex (Saline vs. DA $F_{(1,39)}$: 19.139, $p \leq 0.001$). Eticlopride alone did not alter *zif268* mRNA expression (Saline vs. eticlopride, $F_{(1,39)}$: 1.084, $p = 0.305$). Co-infusion of DA and eticlopride decreases the expression of *zif268* mRNA produced by DA alone (DA vs. DA-eticlopride, $F_{(1,39)}$: 8.836, $p = 0.005$). This expression level was not statistically differentiable from Vehicle treatment.

3.5 Discussion

The unilateral infusion of incremental doses of DA in the caudal caudatoputamen produces a dose-dependent increase in the expression of *zif268* mRNA in the posterior auditory cortex, which confirms that this portion of the striatum is selectively associated with the auditory cortex. This finding is consistent with the participation of the caudatoputamen in processing of the auditory modality (LeDoux et al., 1991). 50 nM DA unilateral injection reproduced the functional activation generated by a sound stimulus of 85 dB.

The effect of DA was also observed in the contralateral auditory cortex, which suggests close communication between the temporal cortices of both hemispheres through trans-callosal cortico-cortical projections (Shepherd, 2013). Importantly, the auditory cortex appears to be selectively activated at -4.4 mm from bregma by an injection of DA in the caudate at -1.8 mm from bregma. This effect denotes a preserved topology in the striato-thalamo-cortical circuit. The precise increase of the expression of *zif268* mRNA in rostro-caudal axis suggests that the effect of DA from the posterior caudate has specific circuits that project into a rostro-caudal level of the auditory cortex.

The functional activation of the temporal cortex affects all cortical layers demonstrating network connectivity within cortical columns. Across the cortical depth, a higher activation level was seen in the input layers, which characterizes this portion of the temporal cortex as a sensory brain region with a predominant input component.

Therefore, in order to functionally demonstrate that this temporal brain region is auditory,

we carried out a laminar analysis after sound or light stimuli. The effects of sound stimulus increased *zif268* mRNA expression in layer III-IV throughout the temporal segment (-3.8 mm to -5.2 mm from bregma) of the cortex, revealing the auditory sensory input of this brain region.

A sound stimulus of 85 dB was able to produce bilateral functional activation of the auditory cortex similar to one caused by DA infusions in the caudatoputamen. A light stimulus did not induce activation significantly higher than the vehicle treatment at any rostro-caudal level. There was no activation in agranular motor cortex after DA infusion in the caudal striatum, suggesting that this portion of the caudal caudatoputamen is more strictly related to auditory rather than motor processing. These findings suggest that the portions covered by our DA manipulations are specifically related to auditory input.

D2R selective antagonist attenuated the effect of striatal DA infusion on functional activation of auditory cortex. The co-infusion of eticlopride, a selective D2R antagonist lowered the expression of *zif268* mRNA to control group levels. D2R antagonist may affect presynaptic DA and glutamate release, as well as, postsynaptic firing of D2R expressing SPNs. Under this assumption, the attenuation produced by eticlopride may take place via postsynaptic D2R by setting SPNs of the indirect pathway in a down functional state, which in turn decreases thalamo-cortical output, rather than through presynaptic D2R, which increases dopaminergic and glutamatergic release, and subsequently increases thalamo-cortical output. Such D2R antagonist effect is consistent with clinical improvement produced by antipsychotics, which are found to be correlated with their D2R affinity (Madras, 2013).

The pharmacological manipulations advanced in this study presents evidence for the involvement of striatal DA transmission in activation of the auditory cortex. Given that similar activation of rat auditory cortex is produced by sound, the present analyses suggest that dopamine affects both direct- and indirect-pathway SPNs that in turn provide intrinsic auditory stimulation. These findings suggest the presence of an auditory striato-pallido-thalamo-cortical circuit, whereby supersensitive postsynaptic D2R signaling in the caudal caudatoputamen induces bilateral activation of the auditory cortex.

We propose this paradigm as a model of endogenous auditory stimulation that may elucidate the biological basis of psychotic symptoms, such as auditory hallucinations. Further study of the projections within this striato-auditory cortical loop is required to describe the nature of this functional relationship. Likewise, a dose-response study is needed to better describe the effects of selective DA antagonists in this paradigm.

Our results characterized the molecular mechanisms of the affected circuit responsible for auditory endogenous activation and provide a strong neurobiological foundation to understanding auditory dysfunction. This model will also facilitate the study of abnormal cortical cadence that resembles schizophrenia like symptoms, thus aligning to the objectives of the National Institutes of Mental Health.

3.6 Financial Disclosures

Support contributed by: USPHS Award MH073930, and funding from the Arizona Biomedical Research Commission.

CHAPTER 4

TRANS-SYNAPTIC RETROGRADE TRACING OF AN AUDITORY CORTICAL CIRCUIT FROM THE POSTERIOR CAUDATOPUTAMEN

4.1 Project summary

Background: Functional studies have reported activation of the auditory cortex during verbal auditory hallucinations, as well as increased dopamine transmission in the caudatoputamen. We have shown that dopamine infusion into the posterior caudatoputamen of the rat dose-dependently activates auditory cortex, as does a sound stimulus, and that co-infusion of a selective D2-like antagonist attenuates this effect. Hence, this work seeks to describe the neuronal connectivity from the posterior caudatoputamen to the auditory cortex through a cortico-striato-thalamo-cortical (CSTC) pathway.

Methods: The circuit was assessed using a retrograde trans-synaptic tracer. We infused PRV-152 in layer IV of the Au of 21 rats. The progression of the infection was evaluated every 12 h post-inoculation. The sensory and striatal pathways were evaluated by chronologically mapping the location of eGFP-expressing neurons and synaptic level of the projections estimated using viral kinetics.

Results: Our results reveal neuronal pathways that connect the auditory cortex and caudatoputamen. We identified direct thalamic projections to auditory cortex from the medial geniculate and the ventral anterior – ventral lateral nuclei. These thalamic

projections depict different rostrocaudal input sources to auditory cortex. Indirect projections to auditory cortex were also identified from ipsilateral posterior caudatoputamen, subthalamic nuclei, and globus pallidus.

Discussion: These neuroanatomical data delineate a neural circuit, which may underlie striatal dopamine-induced functional activation of auditory cortex. We demonstrate here that the posterior caudatoputamen innervates the auditory cortex through a CSTC pathway. We propose that this auditory CSTC pathway represents a biological substrate for intrinsic activation of the auditory cortex, and may be important in the pathophysiology of verbal auditory hallucinations.

4.2 Introduction

The perception of sound is directly associated with the activation of the temporal cortex (Lennox et al., 2000). Normally, an auditory stimulus is transduced into neuronal signals and carried by the sensory auditory pathway from the inner ear to the auditory cortex; however, auditory perception may appear without sound stimulation, causing the human brain to generate an intrinsic perception of sound. (Grassian, 1983). An example of this phenomena is auditory hallucinations, which is characteristic of some psychotic disorders, including schizophrenia. (Allen et al., 2008, Kronmuller et al., 2011). Research on psychotic syndrome has shown an aberrant dopaminergic transmission (Abi-Dargham et al., 1998), more specifically, a hypersensitive dopamine D2-like postsynaptic receptor component that interferes with the modulation of corticostriatal and thalamostriatal projections (Bonci and Hopf, 2005, Surmeier et al., 2007, Madras, 2013).

Based on this knowledge, dopamine antagonists have remained the first line of treatment for symptoms of psychotic disorders, including verbal auditory hallucinations (Buchanan et al., 2002, Lieberman et al., 2005). In addition, animal models for the schizophrenia spectrum of symptoms have revealed that increased dopamine transmission in the posterior caudatoputamen induces activation of the auditory cortex, and that selective D2-like receptor antagonists attenuates this effect (A. Parga, 2012). Consequently, a dopaminergic imbalance in the striatum may generate the intrinsic activation of the auditory cortex in the psychotic brain.

The present study seeks to describe the neuronal circuit that affects the auditory cortex after dopamine manipulations in the posterior caudatoputamen. Previous studies reported functional connectivity between the auditory cortex and the striatum (Hoffman et al., 2011). Nonetheless, the pathway by which the auditory cortex is intrinsically activated has been elusive, perhaps due to its multisynaptic nature. We hypothesized that the posterior caudatoputamen affects the auditory cortex through a striato-thalamo-cortical circuit. We based this hypothesis on the topological organization of the striato-thalamo-cortical loops, which in the posterior aspect of the caudatoputamen project to temporal cortex (Kimura et al., 2004).

4.2.1 Tracing of neuronal circuits

In order to map the striatal projections to the auditory cortex, a multisynaptic tracing technique is necessary; therefore, we implemented the trans-synaptic tracer, pseudorabies virus (PRV) 152. PRV strains have been broadly used to describe

multisynaptic pathways in the brain due to the selective neurotrophic attribute of these viruses (Callaway, 2008, Ugolini, 2010). We used PRV-152 because of its ability to express enhanced green fluorescent protein (eGFP) as an indicator of trans-synaptic retrograde infection, as well as its slower transmission and reduced cytopathic effects (Banfield et al., 2003, Enquist, 2012). The cycle of viral replication takes approximately 12 hours before PRV-152 trans-synaptically infects new neurons. This produces a new level of neurons at a constant rate per synaptic level, which facilitates the mapping of projections.

We aim to detect the projections involved in the neuronal pathway that impinges on the auditory cortex from the caudatoputamen. To discriminate the sequence of viral spread through the circuit levels, the sensory auditory pathway will serve as a canon for the viral spread in the auditory striatal pathway. In this manner, we expect to retrogradely label afferent projections from the ventral posterior and ventral lateral (VA/VL) nuclei as well as the medial geniculate nucleus (MGN) in the first level of neurons; subsequently, the viral detection in striatal structures will demonstrate that further synaptic levels are involved in the striatal input signal to the auditory cortex.

4.3 Experimental design

4.3.1 Animals

Twenty-one adult male Sprague-Dawley rats (250 gm) were group housed in a biosafety level 2 (BSL-2) approved facilities, with HEPA filtered animal isolation units. Animals were maintained in reverse light cycle (12:12 h, lights on at 0900 hours) with

free access to food and water. All experiments were carried out following the guidelines of the National Institute of Health Guide for the Care and Use of Laboratory Animals, and the protocol approved by the University of Arizona Institutional Animal Care and Use Committee.

4.3.2 Virus

Pseudorabies virus 152 was obtained from the Center for Neuroanatomy and Neurotropic Viruses at University of Pittsburgh. Virus was only handled in biosafety cabinet BSL-2. 100 µl aliquots of the neurostock were made in cryovials and after snap-freeze in dry ice stored at -80 C. Individual vials were thawed before intracerebral injections. One aliquot was used to inject up to three animals (100 nl of 7×10^4 pfu/ml) (Card et al., 1999), all excess of virus was inactivated with bleach before being discarded into the appropriate biohazard waste.

4.3.3 Experimental paradigm

To establish the appropriate time of detection (TOD) of the regions of interest (ROI) an initial study was conducted to evaluate the progression of the viral spread during 72 hour after viral infusion at twelve hours intervals. For this purpose, six animals received intracerebral infusion of PRV-152 (see 4.3.4 intracerebral injections) and one animal was assessed at every post-inoculation time (n=1). Once the TOD for the caudatoputamen was found, we evaluated a period from 24 to 48 hours after inoculation at six hours intervals to detect more precisely the viral spread between the second and

fourth synaptic levels. In this later study fifteen animals (n=3) received the same PRV-152 injection and three animals were assessed at every post-inoculation time (Figure 7).

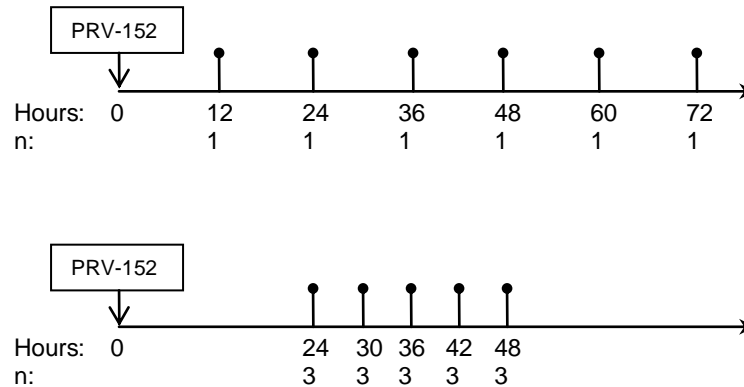


Figure 7. Time line of post-inoculation times evaluated. A) Initial exploratory study 12 – 72 h / 12h. B. complementary study 24 – 48h / 6h to obtain detail on the third synaptic rank.

4.3.4 Intracerebral injections

After pre-anesthesia evaluation in the vivarium, animals were transported to the BSL-2 procedure room. Then, anesthesia was induced with inhaled isoflurane in a protection chamber. Animals were placed in a stereotaxic frame and a surgical window was opened in the scalp to identify the bregma location. The skull was drilled at target coordinates for the right auditory cortex according to rat brain atlas (Ashwell et al., 2007). A 1 μ l Hamilton syringe equipped with 26 gauge cannula was loaded with 0.5 μ l of neurostock and then connected to the infusion pump. The tip of the cannula was placed at the target coordinates (AP -4.3 mm, ML 6.69 mm, DV -4.45 mm) for layer IV of the

secondary auditory cortex, and 100 nl of neurostock were infused at a rate of 10 nl per minute. The cannula was removed five minutes post infusion to prevent reflux. The scalp incision was sutured with staples and the animals were monitored until fully recovered from anesthesia. After recovery, animals were transferred to HEPA filtered animal isolation unit. All animals received the analgesic Buprenorphine 0.06 mL and were followed up every twelve hours post-surgery.

4.3.5 Tissue processing

At the designated post-inoculation time, each animal was euthanized with an intraperitoneal injection of 0.06 ml of 39% pentobarbital sodium solution. Then, the brain was perfused in situ with a transcardial infusion of 100 ml of 10% heparin solution followed by 250 ml of 4% paraformaldehyde, pH: 8.0 at a rate of 25 ml/minute. After the brain was removed from the skull, it was prepared for cryosection by post-fixation in 4% paraformaldehyde at 4 °C for two hours and overnight immersion in 12.5% and 25% phosphate buffer sucrose solution, pH: 7.4 at 4 °C. Each brain was sectioned at 30 µm/section from -1.0 mm to -8.3 mm from bregma; in this manner, we have a sample of each brain every 90 µm in the anterior-posterior axis. The location of the injection sites was confirmed to be within the temporal cortex and at -4.3 mm from bregma. Sequential sections were mounted onto glass slides and coverslipped with ProLong ® Gold antifade reagent, which labels the nucleus of cells with 4',6-diamidino-2-phenylindole (DAPI) for posterior anatomical characterization. Sections were allowed to cure overnight at 4 C° before imaging.

4.3.6 Fluorescent imaging

Each section was imaged at 20X magnification in a Zeiss Axioskope equipped with epifluorescent (488 nm) filter, a motorized stage, and MBF CX 9000 color camera. Images were stitched into a virtual slide using NeuroLucida (MBF-Bioscience, 2012). After background correction, images were flattened and the cells expressing eGFP were detected and marked using an automatic detection object module set to 86% sensitivity, and body size ratio of 40 μm to 450 μm in diameter. Cell markers were confirmed with the live DAPI signal at the microscope.

4.3.7 Analysis of tissue

The virtual slides were superimposed on the rat brain atlas and a rostrocaudal level was assigned to each section. The contours of the section, the thalamus, the hippocampus and the caudatoputamen were traced in a template file. These contours and the cell markers were classified with different user categories according to the hemisphere and the brain region. Then, template files were aligned into an image stack using the center of the section contour and the section middle line as landmarks. A 3D reconstruction of each brain was rendered from the image stack and used for the topographical analysis of the viral spread. Using the 3D reconstruction the stereotaxic coordinates were defined for the center of each ROI (Table 3). Then, we recorded cell counts and calculated minimum distance between the injection site and ROI (Equation 1). The cumulative distance in sequential pathways were also estimated (Equation 2). The

synaptic rank was estimated using the Granstedt's formula (Equation 3) for PRV-152 kinetics.

ROI	Acronyms	mm from Bregma	ROI center (AP/DV/ML)
Auditory Cx	Au	-4.0	-4.5 / 5.0 / 6.5
Anterior & Ventrolateral	VA/VL	-1.8 / -3.4	-2.1 / 6.0 / 1.6
GP Internal	EP	-2.12 / -3.30	-3.1 / 8.0 / 2.8
Subthalamic	STN	-3.60 / -4.30	-3.6 / 8.0 / 2.8
GP External	GP	-1.30 / -3.30	-3.1 / 6.5 / 4.4
Caudate	CP	2.20 / -3.80	-2.3 / 6.0 / 5.4
Medial Geniculate	MGN	-4.52 / -6.30	-6.3 / 6.0 / 3.8
Inferior Colliculus	IC	-7.64 / -9.80	-7.6 / 5.0 / 1.8

Table 6. Rostrocaudal brain segment assessed for ROI: Range distance from Bregma for each ROI and the reference coordinates for distances based on 3D brain reconstructions.

4.3.8 Circuit reconstruction

In order to evaluate the hypothesis of an auditory striatal circuit as a neuronal path from the auditory cortex to the caudatoputamen, the synaptic rank of the regions in the striatal pathway were compared to the sensory pathway. Thus, brain regions with direct projections to the auditory cortex should show eGFP expression concurrently with the MGN, while brain regions with indirect projections to the auditory cortex should be detected subsequently and in accordance with the eGFP expression in the inferior colliculus. The expression of eGFP in every region was measured by evaluating the

average cell counts within each ROI. Next, a heat map was created with the natural logarithm of the average cell counts to identify the TOD for each ROI. A logarithmic transformation was performed to correct for a left skewed distribution of the average cell counts (Equation 4), due to the subtle increase in cell counts in the initial rise of eGFP expression from 24 to 36 hours.

Because the viral spread is mainly delayed by the recruitment of a new synaptic level, we assumed a linear relationship between TOD and synaptic level. Thus, the axonal distance traveled by virions accounts for the remaining variability on the estimation of the synaptic level (Equation 2). In this manner, regions at similar linear distance to the injection site would have equal synaptic level had the virus not spread through the neuronal projections. In contrast, a neuronal path would reveal different synaptic levels for ROI at equal distances from the injection site. Next, the TOD was used to estimate the synaptic rank (Equation 3). ROI were organized following the synaptic rank and grouped for the 24, 30 and 36 hour TOD. We evaluated with ANOVA the main and specific effects in the synaptic rank of these groups in order to differentiate primary and secondary projections to auditory cortex.

Finally, 3D reconstructions were carried out. The virtual slides were then assigned a Z value according to the distance from bregma, which was estimate using the section count and the rat brain atlas as reference. Virtual slides of each brain were saved in a virtual image stack, and each stack was aligned using the contours and center of the sections. Virtual stacks were optimized for rendering in the 3D module by smoothing the 3D volumes for each contour. Volumes then were assigned a transparency percentage to

allow visualization of cellular markers. The 3D reconstructions of the eGFP expressing cells were color coded according to the type of projection (primary or secondary). A video using anaglyph rendering was recorded of each brain turning the reconstruction 360 degrees on the Z-axis.

4.3.9 Mathematics and equations

Equation 1. Distance A – B = $\sqrt{((DV_A - DV_B)^2 + (ML_A - ML_B)^2 + (AP_A - AP_B)^2)}$

A: point of origin, B: target point, DV: dorso-ventral coordinate, ML: medio-lateral coordinate and AP: antero-posterior coordinate.

Equation 2. Distance AB – C = $AB + \sqrt{(((DV_B - DV_C)^2 + (ML_B - ML_C)^2) + (AP_B - AP_C)^2)}$

Equation 3. Synaptic level = $(\text{Time of detection} - (\text{Estimated distance} \div 3.6))/10$

Equation 4. Logarithmic transformation: $X' = \ln(x + 1)$

4.4 Results

Our study evaluated the neuronal input of the auditory cortex to describe additional input pathways to the auditory sensory pathway. We explored the passage of PRV-152 through the circuit in a broad period of 72 hours to estimate the approximate TOD of the ROI.

4.4.1 Time of detection for regions of interest

In this first study, we detected induced eGFP expression after 12 hours postinoculation in the thalamus (Figure 8A) and injection site (Figure 8B), which rapidly peaked around 48 hours in ROI at the third synaptic rank. The spread of PRV-152 throughout the brain revealed brain regions that express eGFP at the same time of the injection site (primary projections) and brain regions that showed a delay in the expression of eGFP (secondary projections). Therefore, in order to discriminate better the secondary input, we evaluated a period of 24 to 48 hours at shorter time intervals. We found a main effect of the TOD between 24 to 36 hours in the synaptic rank of ROI in the ipsilateral hemisphere (ANOVA $F_{(2,9)}$: 16.93, $p < 0.05$) and contralateral hemisphere (ANOVA $F_{(2,9)}$: 355.50, $p < 0.05$).

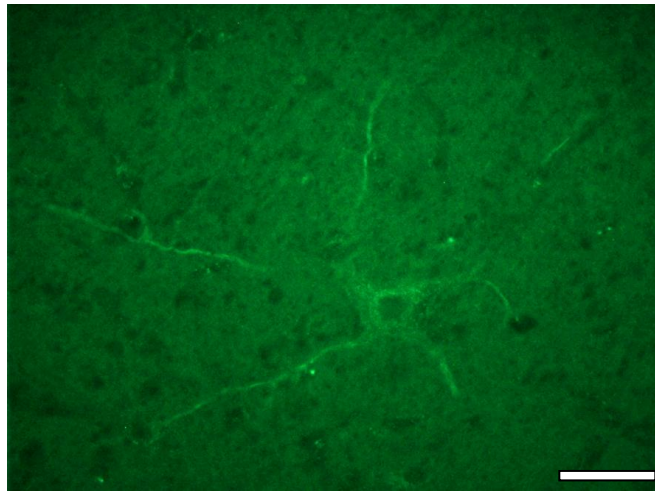


Figure 8A. Cell expressing eGFP in the first synaptic rank; 12 hours postinoculation at 60x. Scale bar depicts 100 μm

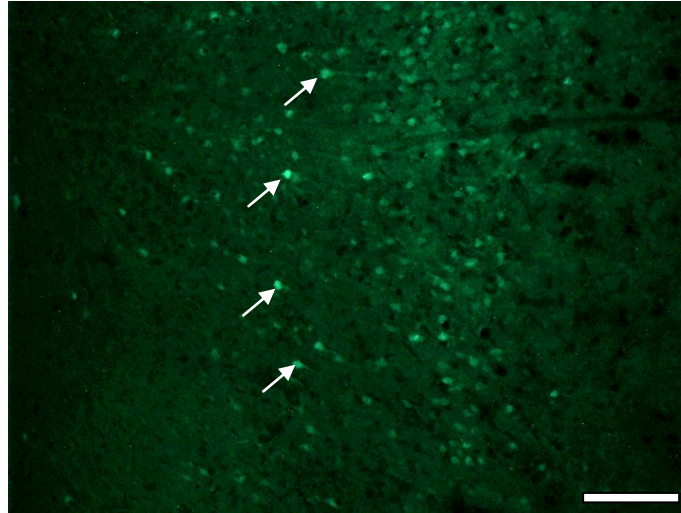


Figure 8B. Injection site and ipsilateral cortex; 24 hours postinoculation at 40x. Scale bar depicts 400 μm

4.4.2 Primary and secondary projections

In the latter study, PRV-152 reached ROI in three main phases (Table 4). We compared the synaptic ranks of these phases to define the ROI of primary and secondary projections. The initial phase expressed eGFP at the same rate as the inoculation site. Thus, the ipsilateral auditory cortex and the thalamus show cell counts after 24 hours postinoculation (Table 4). The simultaneous induction of eGFP expression in the thalamus and the auditory cortex demonstrates direct thalamic input to the injection site. Thalamic projections appeared bilaterally in the VA/VL nuclei and MGN (Figure 8C-D). These initial projections correspond to a second synaptic rank in the sensory and striatal circuit, which denote the thalamo-cortical portion of the circuit. ROI detected at 24 hours have significantly lower synaptic ranks than the ROI detected at 30 and 36 hours (Table

4). In addition to these thalamic nuclei, PRV-152 also spread along the reticular nucleus showing sparse rostrocaudal expression.

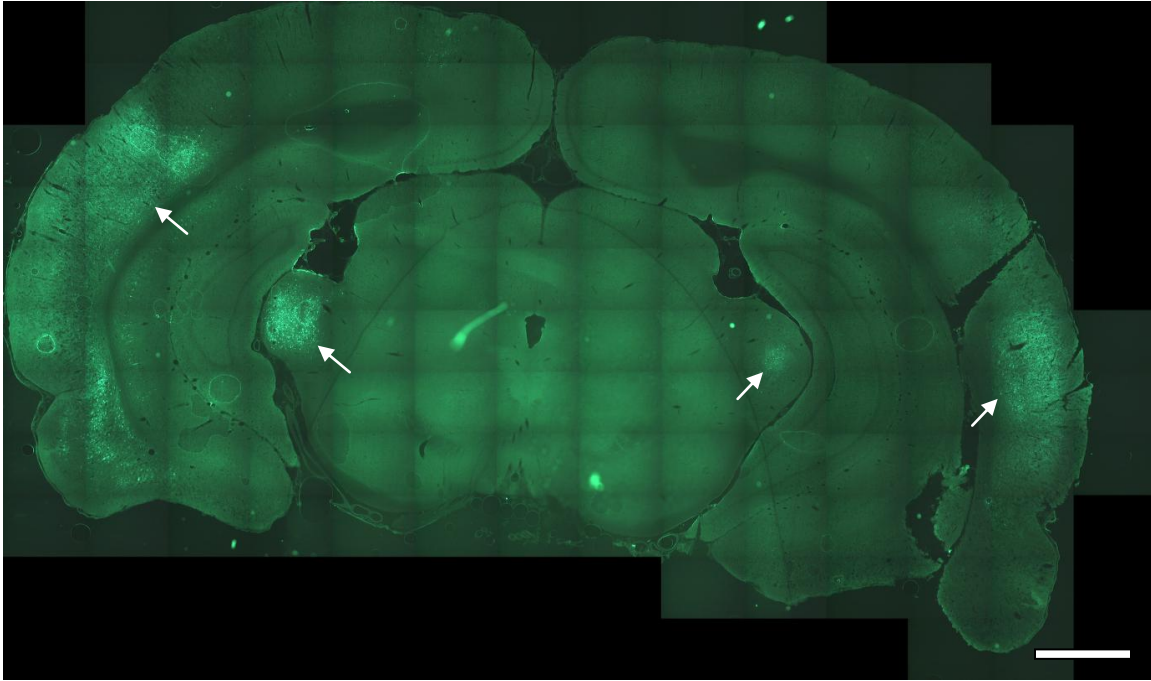


Figure 8C. Posterior projections from the injection site. Virtual slice at 20x in the -6.30 mm level from bregma highlighting primary projections to auditory cortex after 24 hours of PRV-152 inoculation. Scale bar depicts 1.5 mm. White arrows show the bilateral labeling of MGN and auditory cortex.

The second phase of cells expressing eGFP was detected in the ipsilateral entopeduncular nucleus, hippocampus and caudatoputamen (Figure 8E) at 30 hours postinoculation. The synaptic rank of these regions was statistically differentiable from regions detected in the first phase at 24 hours but their ranks did not differ from the regions detected in the third phase at 36 hours postinoculation (Table 4). Therefore, we considered the entopeduncular

nucleus and the caudatoputamen part of the secondary projections in the third synaptic rank.

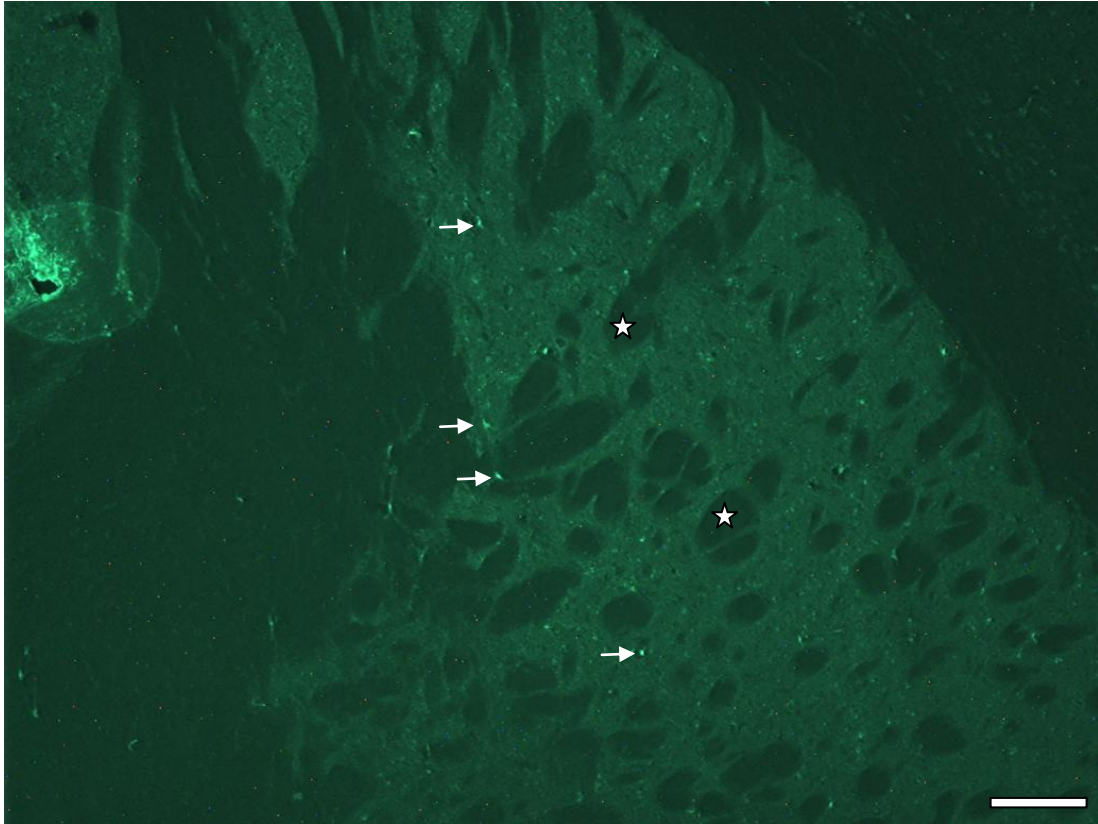


Figure 8D. Cells expressing eGFP in the striatum at 10x. Fluorescent micrograph at -1.8 mm from bregma 36 hours postinoculation of PRV-152. Scale bar depicts 800 μ m. White arrows show eGFP expressing cells. Stars depict fiber tracts.

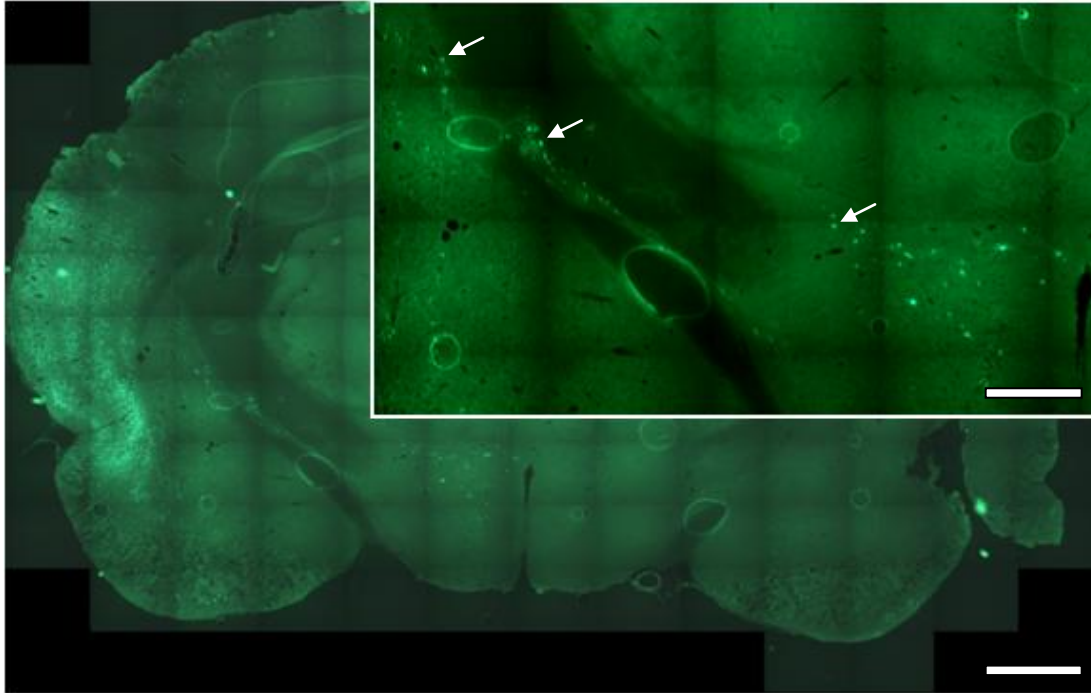


Figure 8E. Anterior projections from the injection site. Virtual slide at 20x in the -3.6 mm level from bregma. Scale bar depicts 1.5 mm. Top right: White arrows depict a close-up of cells expression eGFP in the second and third synaptic level 30 – 36 hours postinoculation. Top left arrow signals the globus pallidus. Bottom right arrow shows eGFP cells in the mesencephalon. Arrow in the middle shows labeling in the entopeduncular nucleus. Scale bar depicts 800 μ m.

In the third phase, PRV spread bilaterally to the IC after 36 hours postinoculation. These neurons correspond to secondary projections of the sensory auditory pathway. Similarly, cells in the globus pallidus and subthalamic nucleus showed bilateral eGFP expression after 36 hours postinoculation (Figure 8E). These indirect projections in both pathways correspond to a third synaptic rank, which have statistically higher synaptic rank than

regions in the first phase (Table 4). Rostral projections in the third phase represent the striato-thalamic portion of the circuit.

		0	24	30	36	42	48	Distance	Synaptic
Ipsilateral	CxAud	0	5.0	4.5	5.9	3.1	7.3	0.0	1.2
	VAVL	0	2.9	2.0	4.3	2.6	4.3	5.5	2.2
	Thalamic	0	2.7	3.1	5.2	2.9	5.0	4.5	2.3
	MGN	0	1.6	0.5	3.3	2.1	5.8	3.4	2.3
	Reticular	0	2.2	2.0	4.1	2.3	4.0	3.0	2.3
	Cortex	0	3.9	3.6	3.9	2.7	8.0	0.0	2.4
	EP	0	0.0	1.1	2.6	1.7	3.6	5.0	2.9
	Hippo	0	0.3	1.5	3.3	2.6	3.7	3.6	2.9
	CP	0	0.0	1.0	3.7	2.4	4.9	2.7	2.9
	IC	0	0.0	0.0	3.5	1.1	1.2	5.7	3.4
	STN	0	0.0	0.5	1.5	0.7	2.0	4.8	3.5
	GP	0	0.0	0.0	2.6	1.6	3.3	2.9	3.5
Contralateral	Reticular	0	2.3	0.8	3.9	2.1	3.9	10.4	2.1
	Hippo	0	1.3	0.5	3.3	2.3	3.6	10.2	2.1
	Thalamic	0	2.9	2.9	5.4	1.7	5.0	9.2	2.1
	VAVL	0	1.8	2.2	4.3	1.8	3.8	8.5	2.2
	Cortex	0	0.7	2.1	4.1	2.7	5.3	13.0	2.6
	CP	0	0.3	1.1	3.3	2.1	4.3	12.1	2.7
	GP	0	0.0	1.5	3.0	1.9	3.1	11.1	2.7
	MGN	0	0.0	0.8	3.4	2.4	3.1	10.5	2.7
	CxAud	0	0.3	0.0	3.6	1.7	5.6	13.0	3.2
	EP	0	0.0	0.5	2.6	0.7	3.6	9.9	3.3
	STN	0	0.0	0.0	1.5	0.3	2.2	9.8	3.3
	IC	0	0.0	0.0	3.9	0.0	1.3	8.9	3.4

Table 7. Logarithm of the average cell counts for brain regions detected from 24 to 48 hours postinoculation. The top heat map corresponds to the ipsilateral hemisphere, and the bottom to the contralateral hemisphere. Heat maps contain the logarithmic transformation of the average cell counts for every brain region according to the time post-inoculation in hours (Top row). Heat maps color code the distribution of average cell

counts along all brain regions and post-inoculation times: Green: above 97.7%, Red: below 2.3% and Yellow: median, other colors correspond to in between values. Distance column shows the triangulated distance from the injection site to each ROI. Synaptic column has the estimated synaptic rank for each ROI. All ROI are listed in order according their synaptic rank (First column).

Ipsilateral Hemisphere F (2, 9) 16.93, p = 0.0009			Contralateral Hemisphere F(2,9) 355.50, p = 0.0000		
	24 h	36 h		24 h	36 h
30 h	0.7833 0.029		30 h	0.55 < 0.0001	
36 h	1.35 0.001	0.5667 0.213	36 h	1.175 < 0.0001	0.625 < 0.0001

Table 8. Comparison of the synaptic ranks between ROI detected at 24, 30 and 36 h.

There is a main effect of TOD in the synaptic rank of ROI within each hemisphere. The F statistic and p values of the ANOVA are shown at the top row for each hemisphere. The comparisons of synaptic rank differences between postinoculation times are shown with p values adjusted with Bonferroni's F test in corresponding cell. P values with statistical significance appear in bold case. In the ipsilateral hemisphere, the group detected at 24 h has lower synaptic ranks than ROI detected at 30 and 36 hours. However, there is no significant difference between the synaptic ranks of ROI detected at 30 and 36 h. In the contralateral hemisphere, synaptic ranks of all groups differ significantly.

4.5 Discussion

The present work demonstrates the neuronal connectivity between the auditory cortex and the posterior aspect of the caudatoputamen. We used the synaptic rank derived from the PRV-152 detection throughout the rat brain to reconstruct the connectivity that impinges on the auditory cortex. Cells infected between 24 and 48 hours revealed the brain regions that send primary and secondary projections to the injection site.

The directionality of the input to the auditory cortex (- 4.2 mm from Bregma) allow us to distinguish caudal projections of the auditory sensory pathway from rostral projections of a striatal origin. These initial retrogradely labeled projections simultaneously appeared in distinctive rostrocaudal portions of the thalamus in the MGN and the VA/VL respectively (Figure 8C). Such sources of direct thalamo-cortical input to the auditory cortex indicate signal integration of auditory processing at this segment of the temporal cortex. A diverse input to auditory cortex also implies that auditory perception involves multiple brain networks in addition to the sensory pathway of auditory modality.

Cortical viral spread around the ipsilateral auditory cortex occurred after 36 hours postinoculation. The viral containment near the injection site up to a third synaptic rank may be due to the dense columnar network, which predominantly sends vertical projections between cortical layers or receive afferent projections from deep brain structures. As a result, less horizontal cortico-cortical projections are characteristic of the auditory (Happel et al., 2014).

The contralateral cortex was detected in the third synaptic rank after bilateral thalamic spread, which suggests a faster passage of PRV-152 across the middle line through the thalamus rather than via trans-callosal projections. This advocates for an important function of the thalamus in the integration of information between hemispheres and also defines the role of cortico-thalamic projections in coordinating auditory cortical input from other brain regions.

The order of ROI following their synaptic rank differed in the contralateral hemisphere from the order in the ipsilateral hemisphere (Table 4). This is most evident in the striatum where ipsilateral input to the ipsilateral thalamus reveals the entopeduncular nucleus as the relay nucleus that participates in the output of the basal ganglia (Atsushi, 2007). In contrast, in the contralateral hemisphere the contralateral globus pallidus was detected earlier than the contralateral entopeduncular nucleus, which suggests that there are projections crossing the middle line at the striato-thalamic portion of the circuit.

The difference in the hemispheric connectivity led us to focus in the ipsilateral hemisphere to distinguish the branching within the third synaptic rank. Thus, we interpreted the detection of the ipsilateral entopeduncular closely followed by the caudatoputamen and the subthalamic nucleus as secondary projections that may depict the convergence of the striatal pathways in the entopeduncular (Figure 8D). If this is so, the detection of the ipsilateral globus pallidus at 36 hours may indicate the subsequent spread of PRV-152 through the ipsilateral indirect striatal pathway.

The delay in striatal induction of eGFP after the thalamic detection indicates that PRV-152 spread through the rostral thalamus before reaching the striatum, which is consistent with a sequential passage of PRV-152 through the circuit. This finding demonstrates the presence of an auditory striato-thalamic-cortical neuronal circuit. Moreover, the detection of secondary projections from the posterior caudatoputamen suggests that the rostral thalamic path further connects with striatal pathways (Smith and Parent, 1986).

We interpret the participation of the striatum in the input auditory networks as an auditory pattern generator involved in the perception of sound, which is congruent with the increased functional connectivity of the thalamus and caudatoputamen reported in the brain of patients with auditory hallucinations (Hoffman et al., 2011). Our findings present groundwork for the mechanism of intrinsic activation of the Au. This new description of the auditory CSTC pathway may explain striatal induced functional activation of the auditory cortex, and therefore provides novel insight into the pathophysiology of verbal auditory hallucinations.

Figure 9A.

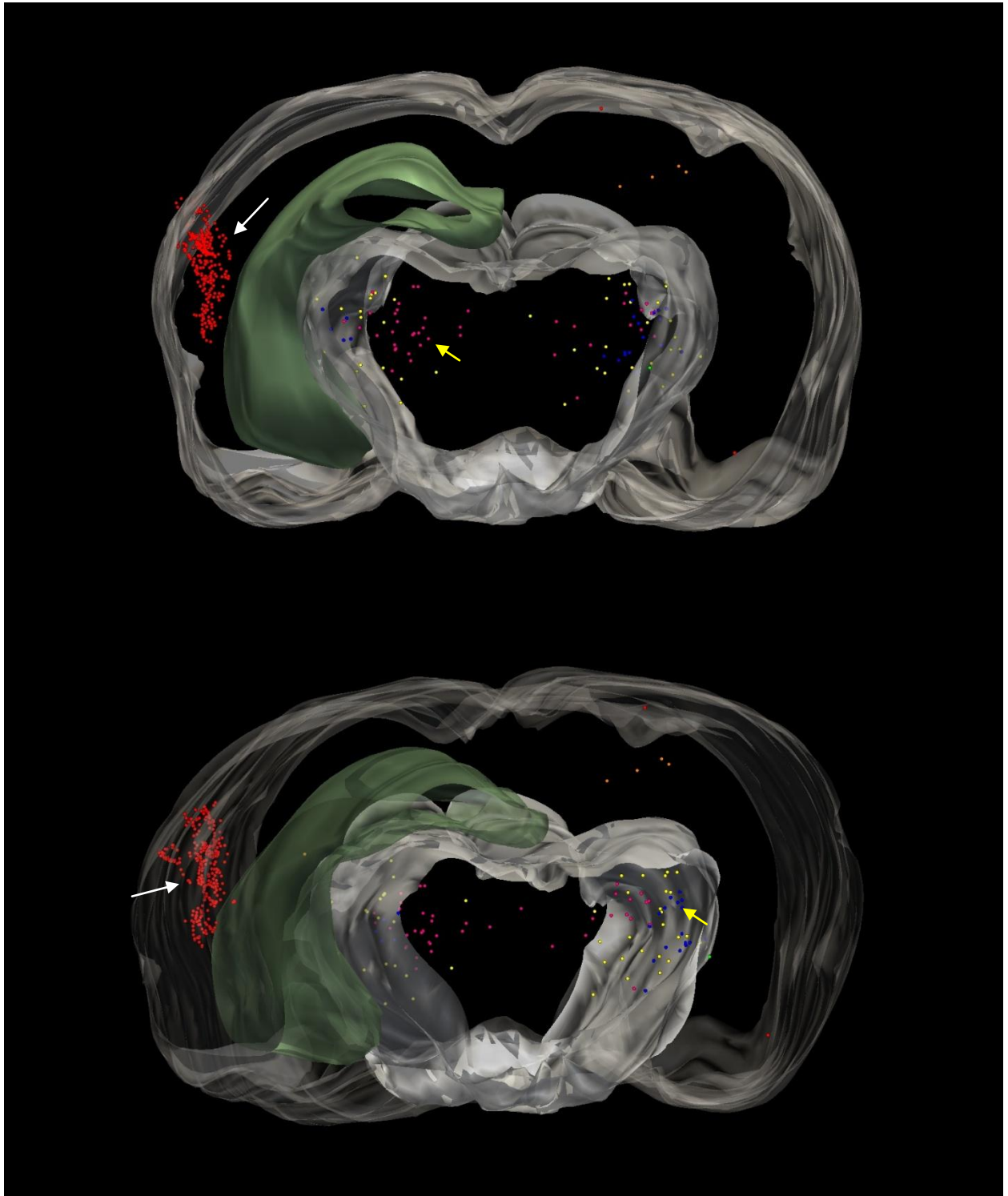


Figure 9B.

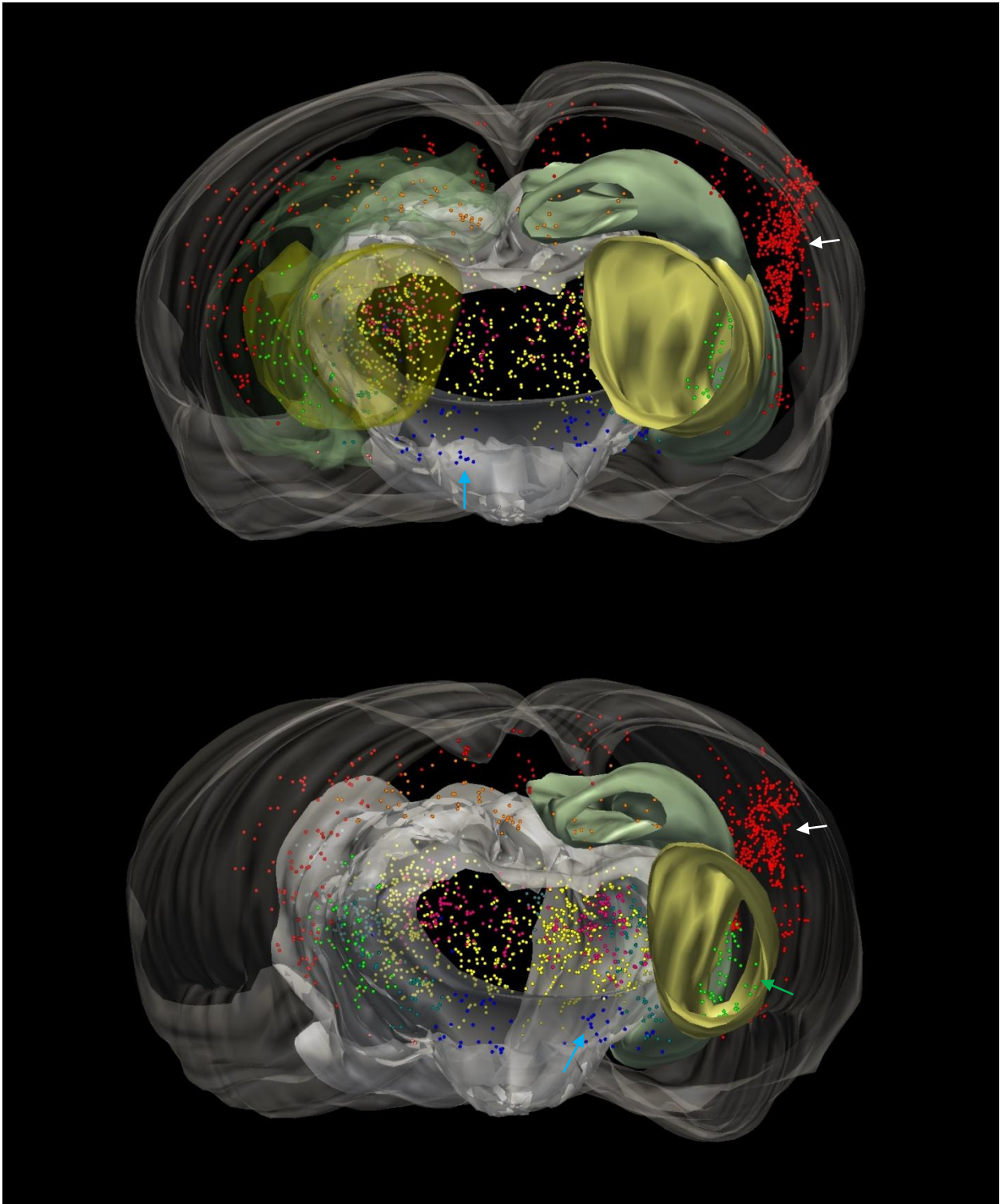


Figure 9C.

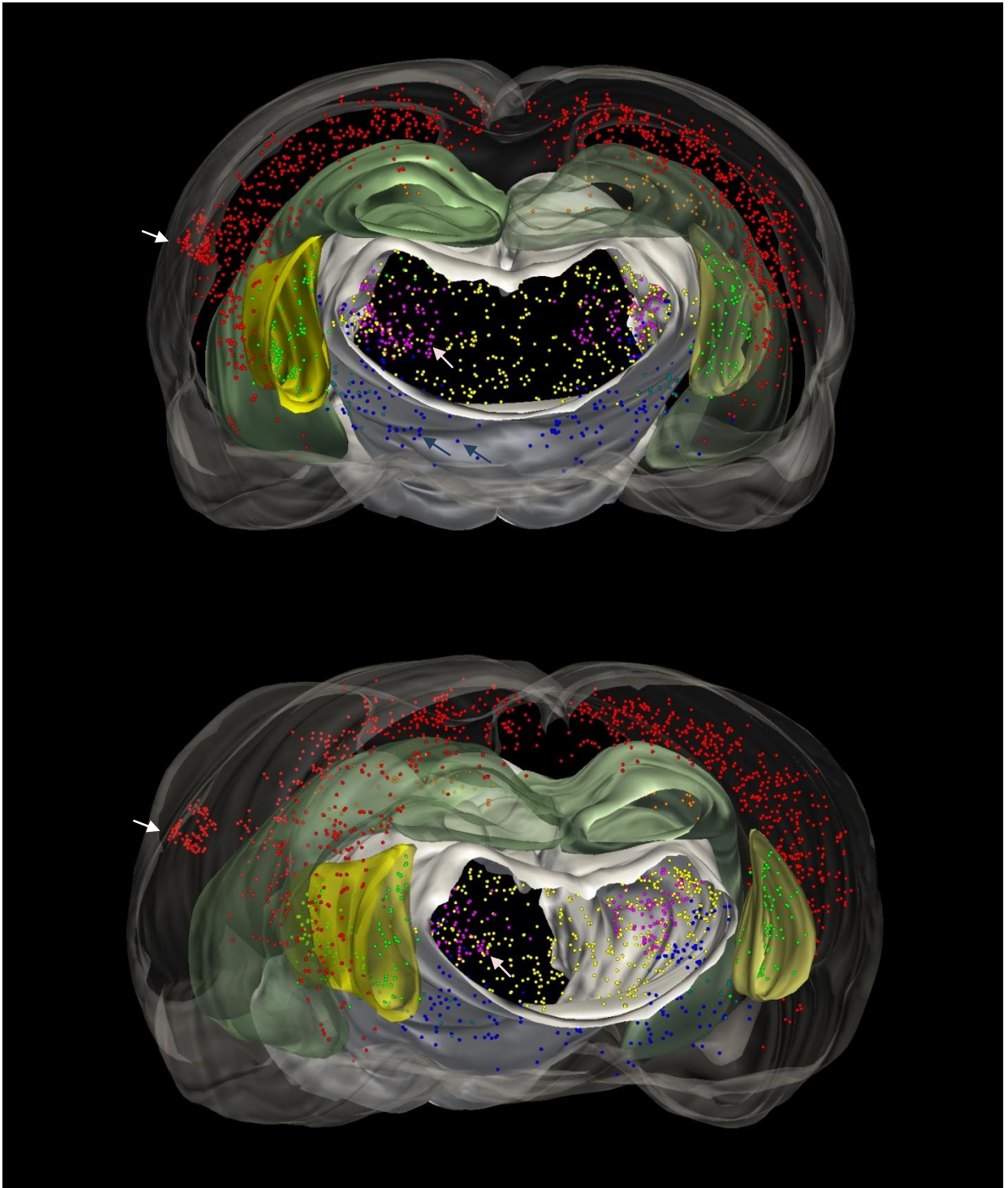


Figure 8. 3D reconstruction of the eGFP expressing cells. Brain reconstructions after A: 24 hours. B: 36 hours and C. 48 hours. The spread over time of PRV-152 through regions can be seen along these reconstructions. A) Shows eGFP expression in the injection site (white arrow) and initial expression in thalamic nuclei (yellow arrows). There are not cells labeled in the mesencephalon or striatum at this time. B) Shows farther extent of the eGFP expression in the injection site (white arrow), and initial expression in contralateral auditory cortex, as well as increased expression in thalamic regions. At this postinoculation time PRV-152 reaches the striatum (See green arrow within the caudatoputamen in yellow) and the mesencephalon (See blue arrow towards the bottom of the brain. C) Farther spread of PRV-152 towards rostral and caudal regions. Cluster of cells can be seen in the thalamic nuclei (See magenta arrow for VA/VL labeling and dark blue arrow for MGN). Brain regions are shown as volume surfaces: Grey: Brain surface. White: diencephalon. derived structures Yellow: Caudatoputamen. Green: Hippocampus. Cells expressing eGFP are shown as dot markers. Direct projections: Bright red: Injection site. Red: Cortex. Yellow: Thalamus. Magenta: VA/VL nuclei. Dark blue: MGN. Indirect projections. Blue: Mesencephalon. Teal: Globus Pallidus. Green: Striatum. Grey: Inferior Colliculus. Orange: Hippocampus.

4.6 Financial disclosures

NIH Grants MH073930 (RPH), P40RR018604 (Center for Neuroanatomy with Neurotropic Viruses)

CHAPTER 5

DISCUSSION

Our findings suggest that enhanced dopaminergic signaling through D2-like receptors in the posterior caudatoputamen enhance the activity of striatal circuits that impinge on the auditory cortex. The effects of dopamine in the brain can be evaluated in the cortex and striatum as these regions express dopamine receptors (Gerfen et al., 1990). However, modulation of information through the CSTC circuit by dopamine takes place at the cortico-striatal, thalamo-striatal, thalamo-cortical and striato-pallidal portion of these circuits. Thus, we will consider each synaptic level.

Dopamine decreases the release of neurotransmitters acting at D2-like presynaptic receptors. For example, this effect may take place either in glutamatergic cortico-striatal or dopaminergic nigro-striatal projections (Bamford et al., 2004). As well as in other input projections into the caudatoputamen that releases other neuromodulators like serotonin. Such mechanism favors a down state of the SPNs of the striatum silencing the output release of glutamate from the thalamus to the cortex.

It is important to note that the release of dopamine has a positive effect on the output flow of the direct and indirect striatal pathways at the thalamic level despite the different effects of dopamine on SPNs modulation. While the glutamatergic signal from cortex may activate or inhibit the striatal pathways, the role of the activation of postsynaptic dopamine receptors is going to increase the firing probability in the thalamus (Bamford et al., 2004). In this manner, the specific action of a co-infusion of D2-like receptor

antagonist reducing the effects on cortex of excessive local dopamine must be postsynaptic; otherwise, the activation of cortex would not be blocked. Therefore, our finding of the alleviation of dopamine-induced auditory cortical activity is interpreted as a postsynaptic D2-like receptor effect.

Another portion of the pathway that may project to the posterior portion of the caudatoputamen consists of thalamo-striatal projections. In this case, the input from the thalamus to the striatum may inhibit the activity of the auditory related circuits (Gerfen and Surmeier, 2011). These projections are glutamatergic and appear to modulate striatal activity through cholinergic and GABAergic interneurons in the striatum (Surmeier et al., 2007). Thus, thalamo-striatal input generates a pause in the activity of SPNs by acting on cholinergic interneurons; specifically, at presynaptic M2 receptors. Furthermore, the effect of thalamo-striatal projections on D2R expressing SPNs may produce an enhanced release of GABA by means of cholinergic response of M1 presynaptic receptors. Taking this into account, the effect of the thalamic feedback to the striatum inhibits activity in the globus pallidus. Such findings are consistent with our finding that the D2-like receptor antagonist acts postsynaptically and decreases the output of the striatum because the effects of thalamo-striatal input on cholinergic cells set the striatal network into a biased state towards D2 activation (Ding et al., 2010).

Enhanced dopamine D2-like receptor transmission on thalamo-cortical glutamatergic projections has been reported in an animal model of schizophrenia (Chun et al., 2014). In this *Drd2* over expression model, D2-like receptors are upregulated affecting the thalamo-cortical release of glutamate. Although our model did not assess the effects of

dopamine on the thalamus, this disruption of transmission at the thalamo-cortical level demonstrates the neuronal connectivity of the thalamus and the auditory cortex, and offers a specific pharmacological model that may be related to auditory activation.

The effects of dopamine on striato-pallidal projections has not been specifically evaluated as most of the dopaminergic basal ganglia input enters at the striatum; however, dopamine release at various levels of the striatal pathways may offer scenarios of neuroplasticity that change the activity of CSTC loops. The fluctuations in the symptomatology of psychotic syndromes may be produced by the involvement of portions of these circuits; hence, striatal plasticity may facilitate or diminish cortical activity. Thus, producing enhanced activation as auditory hallucinations or decreasing function as negative symptomatology. In this manner, the neuroanatomical location of the excessive dopamine transmission defines the spectrum of symptoms according to the function carried out by those neurons.

Laminar analysis of the auditory cortex after excessive dopamine in the caudatoputamen demonstrated activation of input layers III & IV and activation of the cortical segment. The mechanism that enhances auditory cortical activity may be generalized to other cortical regions that involve specific CSTC loops as modulators of cortical activity.

In the auditory system, associative cortices responsible for language like the left superior temporal gyrus and left inferior parietal area could be activated by aberrant function of CSTC circuits generating manifestations of verbal auditory hallucinations (Lennox et al., 2000, Bentaleb et al., 2002). In mammals the auditory cortex maintains a tonotopic

organization derived from the sensory system (Barton et al., 2012). The region activated by dopamine seems to be located posterior to a region of primary auditory sensory input, suggesting that this portion of the auditory cortex may be an associative region. However, the target for the injection of PRV-152 cover a wider area; therefore, producing effects in a striatal and sensory circuits.

Correlating the results of the pharmacological and the neuroanatomical studies, the CSTC loops seem to play an important role interconnecting different cortical regions with a longer reach of connections than cortico-cortical pathways. This has enormous repercussions on integrative functions as the primary cortex receives the sensory input, these CSTC loops submit that information through acquired patterns in the basal ganglia that feedback cortical regions with the relevant interpretation of the signal. Such filtering of information is part of the ability to select and recognize sensory information, which is altered in patients with psychosis.

Although our laminar analysis did not account for the interspersed location of the primary and secondary cortices along the rostrocaudal axis. A better differentiation of the laminar activation can be expected if this factor was considered in future studies. A clear step forward is the description of laminar activation patterns in Happel, 2010 where dopamine produced a sustained sensory cortical activation through positive recurrent feedback in layer II and IV after cortical distal stimulation. In this study, the cortical depth was divided into superficial, input and output layers and the electrical activity was measure after stimulation in the neighbored areas. In this manner, cortico-cortical connections and recurrent connections were assessed showing that the farther the stimulation the more

likely cortical regions are connected through recurrent efferent circuits. In contrast, the closer cortical regions are, the connections seem to reach recording electrode through cortico-cortical connections.

The metabolic activation signaled by increased expression of *zif268* mRNA represents a change in transcription, and therefore a profound effect on neuronal activity. These changes are related to alteration in neuronal plasticity like induction of dendritic growth or long term potentiation of synapses, which are dependent on glutamatergic release. In this manner, the results of our pharmacological studies represent a change in the neuroplasticity of these circuits.

The scenario where different synaptic levels can be affected by neuromodulators in recurrent efferent cortico-striatal loops requires further study of the interactions at each level to dissect the specific effects of dopamine and the function of every group of projections. Further studies are also necessary to clear the complex nature of interneuronal connections onto spiny projecting neurons, and the different network characteristics at every synaptic level.

More detail analysis can be done on the laminar assessment to specify the presence of granular or dysgranular layers. This will provide more accurate measures of the input layers in the cortex.

5.1 Conclusion

Our description of an auditory pathway where known affected brain regions and specific attenuation effects of dopaminergic neurotransmission coincide to regulate the activity of columnar auditory cortical areas offers a first step in the description of recurrent efferent cortico-striatal loops and provides insight to the affected neuronal connectivity related to psychotic symptoms.

The implications for aberrant modulation of CSTC circuits in the integration of information between different brain regions may explain the broad involvement of various brain functions in psychotic syndromes. Furthermore, dopaminergic transmission can modulate corticostriatal projections at different levels of these circuits, which provides more substrates for the generation of psychosis. However, our paradigm suggest the most likely region where dopamine affects CSTC circuits to be the striatum. The therapeutic effects of D2-like receptor antagonist and the evidence from functional studies on the caudate nucleus favor the idea of dysconnection at this portion (Stephan et al., 2006).

When considering the clinical manifestations of psychosis, our results relate to the circuits relevant to auditory function. Nonetheless, similar mechanisms of neuropathology might produce other symptomatology when affecting different brain regions. Perhaps, rostral recurrent efferent circuits are involved in the cognitive symptoms of psychosis. Similarly, caudal recurrent efferent circuits might be related to

visual hallucinations. Negative symptoms respond to different therapeutics, and while correlated to neurological detriment, this symptomatology may be caused by other mechanisms or produced as fluctuations in the function of CSTC circuits decrease the activation of different cortical areas.

LITERATURE CITED

- A. Parga, R. Hammer (2012) Auditory cortical activation after dopamine infusion in caudal caudatoputamen of the rat. *Biological Psychiatry* 71.
- Abi-Dargham A, Gil R, Krystal J, Baldwin RM, Seibyl JP, Bowers M, van Dyck CH, Charney DS, Innis RB, Laruelle M (1998) Increased striatal dopamine transmission in schizophrenia: confirmation in a second cohort. *Am J Psychiatry* 155:761-767.
- Aghajanian GK, Marek GJ (2000) Serotonin model of schizophrenia: emerging role of glutamate mechanisms. *Brain research Brain research reviews* 31:302-312.
- Allen P, Amaro E, Fu CH, Williams SC, Brammer MJ, Johns LC, McGuire PK (2007) Neural correlates of the misattribution of speech in schizophrenia. *Br J Psychiatry* 190:162-169.
- Allen P, Laroi F, McGuire PK, Aleman A (2008) The hallucinating brain: a review of structural and functional neuroimaging studies of hallucinations. *Neuroscience and biobehavioral reviews* 32:175-191.
- Altmann CF, Bledowski C, Wibral M, Kaiser J (2007) Processing of location and pattern changes of natural sounds in the human auditory cortex. *Neuroimage* 35:1192-1200.
- Ashwell KW, Paxinos G, Watson CR (2007) Precerebellar and vestibular nuclei of the short-beaked echidna (*Tachyglossus aculeatus*). *Brain Struct Funct* 212:209-221.
- Atsushi N (2007) Globus pallidus internal segment. In: *Progress in brain research*, vol. 160, pp 135-150.
- Bamford NS, Robinson S, Palmiter RD, Joyce JA, Moore C, Meshul CK (2004) Dopamine modulates release from corticostriatal terminals. *J Neurosci* 24:9541-9552.
- Banfield BW, Kaufman JD, Randall JA, Pickard GE (2003) Development of pseudorabies virus strains expressing red fluorescent proteins: new tools for multisynaptic labeling applications. *J Virol* 77:10106-10112.
- Barbato A (1996) Schizophrenia and Public Health. In: *Nations for Mental Health*, vol. 97.6 Geneva, Switzerland: Division of Mental Health and Prevention of Substance Abuse. World Health Organization.

- Barton B, Venezia JH, Saberi K, Hickok G, Brewer AA (2012) Orthogonal acoustic dimensions define auditory field maps in human cortex. *Proc Natl Acad Sci U S A* 109:20738-20743.
- Battle DE (2013) Diagnostic and Statistical Manual of Mental Disorders (DSM). *CoDAS* 25:191-192.
- Bentaleb LA, Beauregard M, Liddle P, Stip E (2002) Cerebral activity associated with auditory verbal hallucinations: a functional magnetic resonance imaging case study. *Journal of psychiatry & neuroscience*: 27:110-115.
- Bleuler M, Bleuler R (1986) Dementia praecox oder die Gruppe der Schizophrenien: Eugen Bleuler. *Br J Psychiatry* 149:661-662.
- Bloom FE, Costa E, Salmoiraghi GC (1965) Anesthesia and the responsiveness of individual neurons of the caudate nucleus of the cat to acetylcholine, norepinephrine and dopamine administered by microelectrophoresis. *J Pharmacol Exp Ther* 150:244-252.
- Bonci A, Hopf FW (2005) The dopamine D2 receptor: new surprises from an old friend. *Neuron* 47:335-338.
- Buchanan RW, Kreyenbuhl J, Zito JM, Lehman A (2002) The schizophrenia PORT pharmacological treatment recommendations: conformance and implications for symptoms and functional outcome. *Schizophr Bull* 28:63-73.
- Bymaster FP, Felder C, Ahmed S, McKinzie D (2002) Muscarinic receptors as a target for drugs treating schizophrenia. *Current drug targets CNS and neurological disorders* 1:163-181.
- Cachia A, Paillere-Martinot ML, Galinowski A, Januel D, de Beaurepaire R, Bellivier F, Artiges E, Andoh J, Bartres-Faz D, Duchesnay E, Riviere D, Plaze M, Mangin JF, Martinot JL (2008) Cortical folding abnormalities in schizophrenia patients with resistant auditory hallucinations. *Neuroimage* 39:927-935.
- Callaway EM (2008) Transneuronal circuit tracing with neurotropic viruses. *Curr Opin Neurobiol* 18:617-623.
- Card JP, Enquist LW, Moore RY (1999) Neuroinvasiveness of pseudorabies virus injected intracerebrally is dependent on viral concentration and terminal field density. *J Comp Neurol* 407:438-452.
- Choong C, Hunter MD, Woodruff PW (2007) Auditory hallucinations in those populations that do not suffer from schizophrenia. *Curr Psychiatry Rep* 9:206-212.

- Chun S, Westmoreland JJ, Bayazitov IT, Eddins D, Pani AK, Smeyne RJ, Yu J, Blundon JA, Zakharenko SS (2014) Specific disruption of thalamic inputs to the auditory cortex in schizophrenia models. *Science* 344:1178-1182.
- Covington HE, 3rd, Kikusui T, Goodhue J, Nikulina EM, Hammer RP, Jr., Miczek KA (2005) Brief social defeat stress: long lasting effects on cocaine taking during a binge and zif268 mRNA expression in the amygdala and prefrontal cortex. *Neuropsychopharmacology* 30:310-321.
- Crittenden JR, Graybiel AM (2011) Basal Ganglia disorders associated with imbalances in the striatal striosome and matrix compartments. *Front Neuroanat* 5:59.
- Davies LM, Drummond MF (1994) Economics and schizophrenia: the real cost. *The British journal of psychiatry Supplement* 18-21.
- Ding JB, Guzman JN, Peterson JD, Goldberg JA, Surmeier DJ (2010) Thalamic gating of corticostriatal signaling by cholinergic interneurons. *Neuron* 67:294-307.
- E K (1971) *Dementia praecox and paraphrenia.* (Robertson, G. M., ed) New York.
- Enquist JPCaLW (2012) Use and visualization of neuroanatomical transneuronal tracers.
- Font M, Parellada E, Fernandez-Egea E, Bernardo M, Lomena F (2003) [Functional neuroimaging of auditory hallucinations in schizophrenia]. *Actas espanolas de psiquiatria* 31:3-9.
- Freedman R (2003) Schizophrenia. *N Engl J Med* 349:1738-1749.
- Gangarossa G, Espallergues J, Maily P, De Bundel D, de Kerchove d'Exaerde A, Herve D, Girault JA, Valjent E, Krieger P (2013) Spatial distribution of D1R- and D2R-expressing medium-sized spiny neurons differs along the rostro-caudal axis of the mouse dorsal striatum. *Frontiers in neural circuits* 7:124.
- Gerfen CR, Engber TM, Mahan LC, Susel Z, Chase TN, Monsma FJ, Jr., Sibley DR (1990) D1 and D2 dopamine receptor-regulated gene expression of striatonigral and striatopallidal neurons. *Science* 250:1429-1432.
- Gerfen CR, Surmeier DJ (2011) Modulation of striatal projection systems by dopamine. *Annu Rev Neurosci* 34:441-466.
- Grassian S (1983) Psychopathological effects of solitary confinement. *Am J Psychiatry* 140:1450-1454.
- Hammer RP, Jr., Cooke ES (1996) Sensitization of neuronal response to cocaine during withdrawal following chronic treatment. *Neuroreport* 7:2041-2045.

- Happel MF, Deliano M, Handschuh J, Ohl FW (2014) Dopamine-modulated recurrent corticoefferent feedback in primary sensory cortex promotes detection of behaviorally relevant stimuli. *J Neurosci* 34:1234-1247.
- Hoffman RE, Fernandez T, Pittman B, Hampson M (2011) Elevated functional connectivity along a corticostriatal loop and the mechanism of auditory/verbal hallucinations in patients with schizophrenia. *Biol Psychiatry* 69:407-414.
- Hubl D, Koenig T, Strik W, Federspiel A, Kreis R, Boesch C, Maier SE, Schroth G, Lovblad K, Dierks T (2004) Pathways that make voices: white matter changes in auditory hallucinations. *Arch Gen Psychiatry* 61:658-668.
- Johnsen E, Hugdahl K, Fusar-Poli P, Kroken RA, Kompus K (2013) Neuropsychopharmacology of auditory hallucinations: insights from pharmacological functional MRI and perspectives for future research. *Expert review of neurotherapeutics* 13:23-36.
- Kebabian JW, Calne DB (1979) Multiple receptors for dopamine. *Nature* 277:93-96.
- Keefe KA, Gerfen CR (1996) D1 dopamine receptor-mediated induction of zif268 and c-fos in the dopamine-depleted striatum: differential regulation and independence from NMDA receptors. *J Comp Neurol* 367:165-176.
- Kelly RM, Strick PL (2004) Macro-architecture of basal ganglia loops with the cerebral cortex: use of rabies virus to reveal multisynaptic circuits. *Prog Brain Res* 143:449-459.
- Kimura A, Donishi T, Okamoto K, Imbe H, Tamai Y (2007) Efferent connections of the ventral auditory area in the rat cortex: implications for auditory processing related to emotion. *Eur J Neurosci* 25:2819-2834.
- Kimura A, Donishi T, Okamoto K, Tamai Y (2004) Efferent connections of "posterodorsal" auditory area in the rat cortex: implications for auditory spatial processing. *Neuroscience* 128:399-419.
- Knapp M, Mangalore R, Simon J (2004) The global costs of schizophrenia. *Schizophr Bull* 30:279-293.
- Kronmuller KT, von Bock A, Grupe S, Buche L, Gentner NC, Ruckl S, Marx J, Joest K, Kaiser S, Vedder H, Mundt C (2011) Psychometric evaluation of the Psychotic Symptom Rating Scales. *Comprehensive psychiatry* 52:102-108.
- Lahti AC, Weiler MA, Holcomb HH, Tamminga CA, Carpenter WT, McMahon R (2006) Correlations between rCBF and symptoms in two independent cohorts of drug-free patients with schizophrenia. *Neuropsychopharmacology* 31:221-230.

- LeDoux JE, Farb CR, Romanski LM (1991) Overlapping projections to the amygdala and striatum from auditory processing areas of the thalamus and cortex. *Neurosci Lett* 134:139-144.
- Leff J, Sartorius N, Jablensky A, Korten A, Ernberg G (1992) The International Pilot Study of Schizophrenia: five-year follow-up findings. *Psychol Med* 22:131-145.
- Lei W, Jiao Y, Del Mar N, Reiner A (2004) Evidence for differential cortical input to direct pathway versus indirect pathway striatal projection neurons in rats. *J Neurosci* 24:8289-8299.
- Lennox BR, Park SB, Medley I, Morris PG, Jones PB (2000) The functional anatomy of auditory hallucinations in schizophrenia. *Psychiatry Res* 100:13-20.
- Lieberman JA, Stroup TS, McEvoy JP, Swartz MS, Rosenheck RA, Perkins DO, Keefe RS, Davis SM, Davis CE, Lebowitz BD, Severe J, Hsiao JK (2005) Effectiveness of antipsychotic drugs in patients with chronic schizophrenia. *N Engl J Med* 353:1209-1223.
- Lucas G, Bonhomme N, De Deurwaerdere P, Le Moal M, Spampinato U (1997) 8-OH-DPAT, a 5-HT_{1A} agonist and ritanserin, a 5-HT_{2A/C} antagonist, reverse haloperidol-induced catalepsy in rats independently of striatal dopamine release. *Psychopharmacology (Berl)* 131:57-63.
- Madras BK (2013) History of the discovery of the antipsychotic dopamine D₂ receptor: a basis for the dopamine hypothesis of schizophrenia. *Journal of the history of the neurosciences* 22:62-78.
- MBF-Bioscience (2012) *Virtual Tissue Protocol*. (Bioscience, M., ed).
- Moratalla R, Robertson HA, Graybiel AM (1992) Dynamic regulation of NGFI-A (zif268, egr1) gene expression in the striatum. *J Neurosci* 12:2609-2622.
- Nambu A (2007) Globus pallidus internal segment. *Prog Brain Res* 160:135-150.
- Nambu A, Tokuno H, Takada M (2002) Functional significance of the cortico-subthalamo-pallidal 'hyperdirect' pathway. *Neurosci Res* 43:111-117.
- Rauschecker JP, Tian B (2000) Mechanisms and streams for processing of "what" and "where" in auditory cortex. *Proc Natl Acad Sci U S A* 97:11800-11806.
- Rezvani AH, Levin ED (2001) Cognitive effects of nicotine. *Biol Psychiatry* 49:258-267.

- Schreiber R, Dalmus M, De Vry J (2002) Effects of alpha 4/beta 2- and alpha 7-nicotine acetylcholine receptor agonists on prepulse inhibition of the acoustic startle response in rats and mice. *Psychopharmacology (Berl)* 159:248-257.
- Seeman P, Guan HC (2008) Phencyclidine and glutamate agonist LY379268 stimulate dopamine D2High receptors: D2 basis for schizophrenia. *Synapse* 62:819-828.
- Seeman P, Talerico T, Ko F, Tenn C, Kapur S (2002) Amphetamine-sensitized animals show a marked increase in dopamine D2 high receptors occupied by endogenous dopamine, even in the absence of acute challenges. *Synapse* 46:235-239.
- Shepherd GM (2013) Corticostriatal connectivity and its role in disease. *Nat Rev Neurosci* 14:278-291.
- Silbersweig DA, Stern E, Frith C, Cahill C, Holmes A, Grootenck S, Seaward J, McKenna P, Chua SE, Schnorr L, et al. (1995) A functional neuroanatomy of hallucinations in schizophrenia. *Nature* 378:176-179.
- Slotema CW, Blom JD, van Lutterveld R, Hoek HW, Sommer IE (2014) Review of the efficacy of transcranial magnetic stimulation for auditory verbal hallucinations. *Biol Psychiatry* 76:101-110.
- Smith Y, Parent A (1986) Differential connections of caudate nucleus and putamen in the squirrel monkey (*Saimiri sciureus*). *Neuroscience* 18:347-371.
- Stephan KE, Baldeweg T, Friston KJ (2006) Synaptic plasticity and dysconnection in schizophrenia. *Biol Psychiatry* 59:929-939.
- Stephan KE, Friston KJ, Frith CD (2009) Dysconnection in schizophrenia: from abnormal synaptic plasticity to failures of self-monitoring. *Schizophr Bull* 35:509-527.
- Stephane M, Thuras P, Nasrallah H, Georgopoulos AP (2003) The internal structure of the phenomenology of auditory verbal hallucinations. *Schizophr Res* 61:185-193.
- Surmeier DJ, Ding J, Day M, Wang Z, Shen W (2007) D1 and D2 dopamine-receptor modulation of striatal glutamatergic signaling in striatal medium spiny neurons. *Trends Neurosci* 30:228-235.
- Tandon R, Gaebel W, Barch DM, Bustillo J, Gur RE, Heckers S, Malaspina D, Owen MJ, Schultz S, Tsuang M, Van Os J, Carpenter W (2013) Definition and description of schizophrenia in the DSM-5. *Schizophr Res* 150:3-10.
- Ugolini G (2010) Advances in viral transneuronal tracing. *J Neurosci Methods* 194:2-20.

- Warner R (1995) Schizophrenia: a 100-year retrospective. *Am J Psychiatry* 152:1693; author reply 1694-1695.
- Waters FA, Badcock JC, Michie PT, Maybery MT (2006) Auditory hallucinations in schizophrenia: intrusive thoughts and forgotten memories. *Cognitive neuropsychiatry* 11:65-83.
- Weiss AP, Heckers S (1999) Neuroimaging of hallucinations: a review of the literature. *Psychiatry Res* 92:61-74.
- Worley PF, Christy BA, Nakabeppu Y, Bhat RV, Cole AJ, Baraban JM (1991) Constitutive expression of zif268 in neocortex is regulated by synaptic activity. *Proc Natl Acad Sci U S A* 88:5106-5110.